Acknowledgments: We thank Mr. Brent Bell for reviewing the manuscript.

References

1) Guengerich, F. P. and McDonald, J. S.: Applying mechanisms of chemical toxicity to predict drug safety. *Chem. Res. Toxicol.*, **20**: 344–369 (2007).
2) Adams, D. H., Ju, C., Ramaiah, S. K., Uetrecht, J. and Jaeschke, H.: Mechanisms of immune-mediated liver injury. *Toxicol. Sci.*, **115**: 307–321 (2010).
3) Holt, M. P. and Ju, C.: Mechanisms of drug-induced liver injury. *AAPS J.*, **8**: E48–E54 (2006).
4) Lee, W. M.: Drug-induced hepatotoxicity. *N. Engl. J. Med.*, **349**: 474–485 (2003).
5) Guengerich, F. P.: Cytochrome P-450 3A4: regulation and role in drug metabolism. *Annu. Rev. Pharmacol. Toxicol.*, **39**: 1–17 (1999).
6) Hosomi, H., Fukami, T., Iwamura, A., Nakajima, M. and Yokoi, T.: Development of a highly sensitive cytotoxicity assay system for CYP3A4-mediated metabolic activation. *Drug Metab. Dispos.*, **39**: 1388–1395 (2011).
7) Eliasson, E., Gardner, I., Hume-Smith, H., de Waziers, I., Beaune, P. and Kenna, J. G.: Interindividual variability in P450-dependent generation of neoantigens in halothane hepatitis. *Chem. Biol. Interact.*, **116**: 123–141 (1998).
8) Sanderson, J. P., Naisbitt, D. J., Farrell, J., Ashby, C. A., Tucker, M. J., Rieder, M. J., Pirmohamed, M., Clarke, S. E. and Park, B. K.: Sulfamethoxazole and its metabolite nitroso sulfamethoxazole stimulate dendritic cell costimulatory signaling. *J. Immunol.*, **178**: 5533–5542 (2007).
9) Higuchi, S., Kobayashi, M., Yano, A., Tsuneyama, K., Fukami, T., Nakajima, M., *et al.*: Involvement of Th2 cytokines in the mouse model of flutamide-induced acute liver injury. *J. Appl. Toxicol.*, **32**: 815–822 (2011).
10) Higuchi, S., Kobayashi, M., Yoshikawa, Y., Tsuneyama, K., Fukami, T., Nakajima, M., *et al.*: IL-4 mediates dicloxacillin-induced liver injury in mice. *Toxicol. Lett.*, **200**: 139–145 (2011).
11) Kobayashi, M., Higuchi, S., Mizuno, K., Tsuneyama, K., Fukami, T., Nakajima, M., *et al.*: Interleukin-17 is involved in α-naphthylisothiocyanate-induced liver injury in mice. *Toxicology*, **275**: 50–57 (2010).
12) Kobayashi, E., Kobayashi, M., Tsuneyama, K., Fukami, T., Nakajima, M. and Yokoi, T.: Halothane-induced liver injury is mediated by interleukin-17 in mice. *Toxicol. Sci.*, **111**: 302–310 (2009).
13) Toyoda, Y., Endo, S., Tsuneyama, K., Miyashita, T., Yano, A., Fukami, T., *et al.*: Mechanism of exacerbative effect of progesterone on drug-induced liver injury. *Toxicol. Sci.*, **126**: 16–27 (2011).
14) Toyoda, Y., Miyashita, T., Endo, S., Tsuneyama, K., Fukami, T., Nakajima, M., *et al.*: Estradiol and progesterone modulate halothane-induced liver injury in mice. *Toxicol. Lett.*, **204**: 17–24 (2011).
15) Bradham, C. A., Plümpe, J., Manns, M. P., Brenner, D. A. and Trautwein, C.: Mechanisms of hepatic toxicity. I. TNF-induced liver injury. *Am. J. Physiol.*, **275**: G387–G392 (1998).
16) Baggiolini, M., Dewald, B. and Moser, B.: Interleukin-8 and related chemotactic cytokines—CXC and CC chemokines. *Adv. Immunol.*, **55**: 97–179 (1994).
17) Leonard, E. J., Yoshimura, T., Tanaka, S. and Raffeld, M.: Neutrophil recruitment by intradermally injected neutrophil attractant/activation protein-1. *J. Invest. Dermatol.*, **96**: 690–694 (1991).
18) You, Q., Cheng, L., Reilly, T. P., Wegmann, D. and Ju, C.: Role of neutrophils in a mouse model of halothane-induced liver injury. *Hepatology*, **44**: 1421–1431 (2006).
19) Edling, Y., Sivertsson, L. K., Butura, A., Ingelman-Sundberg, M. and Ek, M.: Increased sensitivity for troglitazone-induced cytotoxicity using a human in vitro co-culture model. *Toxicol. In Vitro*, **23**: 1387–1395 (2009).
20) Edling, Y., Sivertsson, L., Andersson, T. B., Porsmyr-Palmertz, M. and Ingelman-Sundberg, M.: Pro-inflammatory response and adverse drug reactions: mechanisms of action of ximelagatran on chemokine and cytokine activation in a monocyte in vitro model. *Toxicol. In Vitro*, **22**: 1588–1594 (2008).
21) Mizuno, K., Toyoda, Y., Fukami, T., Nakajima, M. and Yokoi, T.: Stimulation of pro-inflammatory responses by mebendazole in human monocytic THP-1 cells through an ERK signaling pathway. *Arch. Toxicol.*, **85**: 199–207 (2011).
22) Mizuno, K., Fukami, T., Toyoda, Y., Nakajima, M. and Yokoi, T.: Terbinafine stimulates the pro-inflammatory responses in human monocytic THP-1 cells through an ERK signaling pathway. *Life Sci.*, **87**: 537–544 (2010).
23) Sakaguchi, H., Ashikaga, T., Miyazawa, M., Yoshida, Y., Ito, Y., Yoneyama, K., *et al.*: Development of an in vitro skin sensitization test using human cell lines; human cell line activation test (h-CLAT). II. An inter-laboratory study of the h-CLAT. *Toxicol. In Vitro*, **20**: 774–784 (2006).
24) Becker, D., Kolde, G., Reske, K. and Knop, J.: An in vitro endocytotic activation of murine epidermal Langerhans cells under the influence of contact allergens. *J. Immunol. Methods*, **169**: 195–204 (1994).
25) Miyazawa, M., Ito, Y., Yoshida, Y., Sakaguchi, H. and Suzuki, H.: Phenotypic alterations and cytokine production inTHP-1 cells in response to allergens. *Toxicol. In Vitro*, **21**: 428–437 (2007).
26) Ohyama, K., Nakajima, M., Nakamura, S., Shimada, N., Yamazaki, H. and Yokoi, T.: A significant role of human cytochrome P450 2C8 in amiodarone N-deethylation: an approach to predict the contribution with relative activity factor. *Drug Metab. Dispos.*, **28**: 1303–1310 (2000).
27) Yoshida, Y., Sakaguchi, H., Ito, Y., Okuda, M. and Suzuki, H.: Evaluation of the skin sensitization potential of chemicals using expression of co-stimulatory molecules, CD54 and CD86, on the naïve THP-1 cell line. *Toxicol. In Vitro*, **17**: 221–228 (2003).
28) Gottschall, D. W., Theodorides, V. J. and Wang, R.: The metabolism of benzimidazole anthelmintics. *Parasitol. Today*, **6**: 115–124 (1990).
29) Rawden, H. C., Kokwaro, G. O., Ward, S. A. and Edwards, G.: Relative contribution of cytochromes P-450 and flavin-containing monoxygenases to the metabolism of albendazole by human liver microsomes. *Br. J. Clin. Pharmacol.*, **49**: 313–322 (2000).
30) McCarthy, T. C., Pollak, P. T., Hanniman, E. A. and Sinal, C. J.: Disruption of hepatic lipid homeostasis in mice after amiodarone treatment is associated with peroxisome proliferator-activated receptor-α target gene activation. *J. Pharmacol. Exp. Ther.*, **311**: 864–873 (2004).
31) O'Brien, P. J., Irwin, W., Diaz, D., Howard-Cofield, E., Krejsa, C. M., Slaughter, M. R., *et al.*: High concordance of drug-induced human hepatotoxicity with in vitro cytotoxicity measured in a novel cell-based model using high content screening. *Arch. Toxicol.*, **80**: 580–604 (2006).
32) Trompezinski, S., Migdal, C., Tailhardat, M., Le Varlet, B., Courtellemont, P., Haftek, M., *et al.*: Characterization of early events involved in human dendritic cell maturation induced by sensitizers: cross talk between MAPK signalling pathways. *Toxicol. Appl. Pharmacol.*, **230**: 397–406 (2008).
33) Mitjans, M., Viviani, B., Lucchi, L., Galli, C. L., Marinovich, M. and Corsini, E.: Role of p38 MAPK in the selective release of IL-8 induced by chemical allergen in naive THP-1 cells. *Toxicol. In Vitro*, **22**: 386–395 (2008).
34) Waldhauser, K. M., Torok, M., Ha, H. R., Thomet, U., Konrad,

D., Brecht, K., *et al.*: Hepatocellular toxicity and pharmacological effect of amiodarone and amiodarone derivatives. *J. Pharmacol. Exp. Ther.*, 319: 1413–1423 (2006).
35) Breuer, H. W., Bossek, W., Haferland, C., Schmidt, M., Neumann, H. and Gruszka, J.: Amiodarone-induced severe hepatitis mediated by immunological mechanisms. *Int. J. Clin. Pharmacol. Ther.*, 36: 350–352 (1998).
36) Lewis, J. H., Mullick, F., Ishak, K. G., Ranard, R. C., Ragsdale, B., Perse, R. M., *et al.*: Histopathologic analysis of suspected amiodarone hepatotoxicity. *Hum. Pathol.*, 21: 59–67 (1990).
37) Zahno, A., Brecht, K., Morand, R., Maseneni, S., Török, M., Lindinger, P. W., *et al.*: The role of CYP3A4 in amiodarone-associated toxicity on HepG2 cells. *Biochem. Pharmacol.*, 81: 432–441 (2011).
38) Futamura, Y.: Effect of amiodarone on cytokine release and on enzyme activities of mouse alveolar macrophages, bone marrow macrophages, and blood monocytes. *J. Toxicol. Sci.*, 21: 125–134 (1996).
39) Stäubli, M., Bircher, J., Galeazzi, R. L., Remund, H. and Studer, H.: Serum concentrations of amiodarone during long term therapy. Relation to dose, efficacy and toxicity. *Eur. J. Clin. Pharmacol.*, 24: 485–494 (1983).
40) Lalloz, M. R., Byfield, P. G., Greenwood, R. M. and Himsworth, R. L.: Binding of amiodarone by serum proteins and the effects of drugs, hormones and other interacting ligands. *J. Pharm. Pharmacol.*, 36: 366–372 (1984).
41) Berger, Y. and Harris, L.: Pharmacokinetics. In: Harris, L. and Roncucci, R. (eds.): *Amiodarone: Pharmacology, Pharmacokinetics, Toxicology, and Clinical Effects*, Paris, Medecine et Science Internationales, 1986, pp. 45–98.
42) Latini, R., Tognoni, G. and Kates, E. R.: Clinical pharmacokinetics of amiodarone. *Clin. Pharmacokinet.*, 9: 136–156 (1984).
43) Ha, H. R., Bigler, L., Wendt, B., Maggiorini, M. and Follath, F.: Identification and quantitation of novel metabolites of amiodarone in plasma of treated patients. *Eur. J. Pharm. Sci.*, 24: 271–279 (2005).
44) Ohyama, K., Nakajima, M., Suzuki, M., Shimada, N., Yamazaki, H. and Yokoi, T.: Inhibitory effects of amiodarone and its N-deethylated metabolite on human cytochrome P450 activities: prediction of in vivo drug interactions. *Br. J. Clin. Pharmacol.*, 49: 244–253 (2000).

1521-009X/12/4008-1620–1627$25.00
DRUG METABOLISM AND DISPOSITION

DMD 40:1620–1627, 2012

Vol. 40, No. 8
45625/3785291

Preparation of a Specific Monoclonal Antibody against Human UDP-Glucuronosyltransferase (UGT) 1A9 and Evaluation of UGT1A9 Protein Levels in Human Tissues

Shingo Oda, Miki Nakajima, Masahiko Hatakeyama, Tatsuki Fukami, and Tsuyoshi Yokoi

Drug Metabolism and Toxicology, Faculty of Pharmaceutical Sciences, Kanazawa University, Kakuma-machi, Kanazawa, Japan (S.O., M.N., T.F., T.Y.); and CLEA Japan, Kitayama, Fujinomiya, Shizuoka, Japan (M.H.)

Received March 8, 2012; accepted May 22, 2012

ABSTRACT:

Glucuronidation is a major detoxification pathway of drugs and xenobiotics that are catalyzed by the UDP-glucuronosyltransferase (UGT) superfamily. Determination of the protein levels of the individual UGT isoforms in human tissues is required for the successful extrapolation of in vitro metabolic data to in vivo clearance. Most previous studies evaluating UGT isoform expression were limited to the mRNA level because of the high degree of amino acid sequence homology between UGT isoforms that has hampered the availability of isoform-specific antibodies. In this study, we generated a peptide-specific monoclonal antibody against human UGT1A9. We demonstrated that this antibody does not cross-react with the other UGT1A isoforms including UGT1A7, UGT1A8, and UGT1A10 and shows a high degree of amino acid sequence similarity with UGT1A9. Using this antibody, we found that UGT1A9 protein is expressed in the kidney and the liver but not in the jejunum or the ileum, consistent with previous reports of mRNA expression. In a panel of 20 individual human livers, the UGT1A9 protein levels exhibited 9-fold variability. It is noteworthy that the relative UGT1A9 protein levels were not correlated with the UGT1A9 mRNA level ($r = -0.13$), like other UGT isoforms reported previously, suggesting the importance of evaluating UGT isoform expression at protein levels. In conclusion, we generated a specific monoclonal antibody against UGT1A9 and evaluated the distribution and relative expression levels of the UGT1A9 protein in human tissues. This antibody may serve as a useful tool for further studies of UGT1A9 to evaluate its physiological, pharmacological, and toxicological roles in human tissues.

Introduction

UDP-glucuronosyltransferases (UGTs) are a family of phase II drug-metabolizing enzymes that play key roles in the metabolism of endogenous and exogenous compounds. UGTs mediate the transfer of glucuronic acid from UDP-glucuronic acid to hydrophobic compounds, facilitating their elimination via bile and urine. Whereas glucuronidation usually inactivates biologically active molecules, there are exceptions, such as morphine and retinoic acids, which are converted to pharmacologically active glucuronides (Shimomura et al., 1971; Formelli et al., 1996).

Human UGTs are classified by evolutionary divergence into three subfamilies, including UGT1A, UGT2A, and UGT2B (Mackenzie et al., 2005). The human *UGT1A* gene cluster is located on chromosome 2q37 and contains multiple unique first exons, as well as the conserved exons 2 to 5, which can give rise to nine kinds of functional UGT1A isoforms, including UGT1A1, UGT1A3, UGT1A4, UGT1A5, UGT1A6, UGT1A7, UGT1A8, UGT1A9, and UGT1A10 (Gong et al., 2001). Among them, UGT1A1, UGT1A3, UGT1A4, UGT1A6, and UGT1A9 are expressed in liver, whereas UGT1A7, UGT1A8, and UGT1A10 are predominantly expressed in the gastrointestinal tract (Strassburg et al., 1997, 2000). In these tissues, UGT enzymes are induced by various endogenous and exogenous compounds (Sutherland et al., 1993; Mackenzie et al., 2003). Genetic polymorphisms have been reported for most human *UGT* genes (Guillemette, 2003). These features would be the possible reasons for interindividual variability of expression level and enzymatic activity, which may be associated with the interindividual variability of drug efficacy and toxicity.

Variability of UGT expression can be evaluated by measuring enzyme activity in vitro using specific substrates. However, substrates that are specifically metabolized by a single UGT isoform are limited because of the broad and overlapping substrate specificities of UGTs. Inappropriate selection of substrates may lead to misevaluation. An alternative approach is to measure mRNA levels of individual UGT isoforms. Indeed, earlier studies evaluated the interindividual difference in the expression or tissue distribution of UGT isoforms at the mRNA level (Strassburg et al., 2000; Izukawa et al., 2009; Ohno and Nakajin, 2009). However, we and other research groups reported that certain individual UGT mRNA levels correlate poorly with their respective protein levels (Izukawa et al., 2009; Ohtsuki et al., 2012). Therefore, it should be noted that the mRNA levels might not necessarily reflect the actual UGT protein levels. Immunochemical techniques are the most conventional approaches for the assessment of

Article, publication date, and citation information can be found at http://dmd.aspetjournals.org.
http://dx.doi.org/10.1124/dmd.112.045625.

ABBREVIATIONS: UGT, UDP-glucuronosyltransferase; HEK, human embryonic kidney; Endo H, endoglycosidase H; PNGase F, peptide:*N*-glycosidase F; HNF, hepatocyte nuclear factor; PAGE, polyacrylamide gel electrophoresis; HLM, human liver microsomes; miRNA, microRNA.

protein levels. However, this approach is limited by the specificity of available antibodies. At present, specific antibodies for human UGT isoforms are only commercially available for UGT1A1 and UGT1A6. Antibodies against UGT1A4 and UGT1A9 are also available for purchase, but their specificity is not guaranteed. Because UGT1A9 exhibits as high as 88 to 94% amino acid homology with UGT1A7, UGT1A8, and UGT1A10, it is a great challenge to generate a specific antibody against UGT1A9. Indeed, the antibody against UGT1A9 prepared by Girard et al. (2004) exhibits cross-reactivity against UGT1A7, UGT1A8, and UGT1A10. In this study, we generated a highly specific monoclonal antibody against human UGT1A9 to evaluate the variability of UGT1A9 protein levels in a panel of human liver samples by Western blot analysis.

Materials and Methods

Materials. Recombinant human UGT1A1, UGT1A3, UGT1A4, UGT1A6, UGT1A7, UGT1A8, UGT1A9, and UGT1A10 expressed in baculovirus-infected insect cells (Supersomes) and human liver microsomes (a pooled sample, $n = 50$) were purchased from BD Gentest (Woburn, MA). Human kidney microsomes (a pooled sample, $n = 6$, as well as three individual donors), human jejunum microsomes (a pooled sample, $n = 10$), and human ileum microsomes (a pooled sample, $n = 4$) were purchased from Tissue Transformation Technologies (Edison, NJ). Human liver samples from 14 individual donors were supplied by the National Disease Research Interchange (Philadelphia, PA) through the Human and Animal Bridging Research Organization (Chiba, Japan), and those from 6 Japanese donors were obtained from autopsy materials that were discarded after pathological investigation (Izukawa et al., 2009). Microsomes were prepared as described previously (Tabata et al., 2004). The use of the human livers was approved by the ethics committees of Kanazawa University (Kanazawa, Japan) and Iwate Medical University (Morioka, Japan). A human embryonic kidney-derived cell line (HEK293) stably expressing UGT1A9 was established previously in our laboratory (Fujiwara et al., 2007). A human hepatocellular carcinoma cell line (HepG2), an immortalized human kidney tubular epithelial cell line (HK-2), and a human breast adenocarcinoma cell line (MCF-7) were obtained from American Type Culture Collection (Manassas, VA) and cultured as described previously (Nakamura et al., 2008). Endoglycosidase H (Endo H) and peptide:*N*-glycosidase F (PNGase F) were purchased from New England Biolabs (Ipswich, MA). A goat anti-human hepatocyte nuclear factor (HNF) 1α (C-19) polyclonal antibody and mouse anti-β-actin monoclonal antibody (C-14) were purchased from Santa Cruz Biotechnology, Inc. (Santa Cruz, CA). All the other reagents were of the highest grade commercially available.

Preparation of Monoclonal Antibody against UGT1A9. The selection of antigenic peptide, peptide synthesis, and keyhole limpet hemocyanin conjugation was performed by Biogate (Gifu, Japan). Hydrophilicity, secondary structure, surface probability, and antigenicity were considered in the designation of the antigenic peptide sequence as follows. The hydrophilicity was evaluated by the method of Hopp and Woods (1981). The secondary structure was evaluated by the method of Chou and Fasman (1974) and the method of Robson (Garnier et al., 1978) using GENETYX-MAC software (Software Development, Tokyo, Japan). The surface probability was evaluated by the method of Emini et al. (1985). Antigenicity was evaluated by the method of Welling et al. (1985) and the method of Parker et al. (1986) using original software. The designed peptide sequence was subjected to BLASTP search (http://www.ncbi.nlm.nih.gov/blast/) to screen its homology with known protein sequences. Based on these evaluations, the sequence, DREFKAFAHAQWKAQVRSIYSLLMG-SYNDIFD, which corresponds to the residues 87 to 118 of UGT1A9, was raised as a candidate peptide. At the N terminus of the synthesized peptide, a cysteine residue was added to facilitate conjugation to the carrier protein, keyhole limpet hemocyanin. The mouse monoclonal antibody against the peptide was prepared by CLEA Japan (Tokyo, Japan) using a standard protocol. The hybridomas producing the antibodies were screened by enzyme-linked immunosorbent assay with the synthesized peptide. Reactivity and specificity of antibody clones were evaluated by Western blotting as described below. A clone that specifically reacted with UGT1A9 was expanded by intraperitoneal injection into mineral oil-primed mice. Monoclonal antibodies from mouse ascitic fluids were partially purified by precipitation with 33% ammonium sulfate.

SDS-PAGE and Western Blot Analysis. For the analysis of UGT1A9, UGT Supersomes (2.5 μg), total cell homogenates from HEK293 cells expressing UGT1A9 (40 μg), or microsomes from human tissues (15 μg), mouse or rat liver, and human cell lines (30 μg) were separated by 10% SDS-PAGE and transferred to Protran nitrocellulose membranes (Whatman GmbH, Dassel, Germany). The quantity of protein loaded onto gels was decided to be in the range showing linearity. In some cases, human liver microsomes or recombinant UGT1A9 proteins were treated with Endo H, which cleaves the bond between two *N*-acetylglucosamines directly proximal to the asparagine residue, or PNGase F, which cleaves the bond between asparagine and the *N*-acetylglucosamine residue. The enzyme sources were adjusted to a 2 mg/ml protein concentration with a denaturing buffer containing a final concentration of 0.5% SDS and 40 mM dithiothreitol and subsequently were denatured at 95°C for 10 min. An aliquot [2.5 μg of UGT1A9 Supersomes, 40 μg of UGT1A9 expressed in HEK293 cells, and 30 μg of human liver microsomes (HLM)] was incubated with 250 U of Endo H in 50 mM sodium citrate buffer (pH 5.5) or 500 U of PNGase F in 50 mM sodium phosphate buffer (pH 7.5) containing 1% NP-40 at 37°C for 1 h.

For the analysis of HNF1α, 50 μg of human liver homogenates were separated by 7.5% SDS-PAGE and transferred to a polyvinylidene difluoride Immobilon-P membrane (Millipore Corporation, Billerica, MA). For the analysis of β-actin, 10 μg of human liver microsomes or homogenates were separated by 7.5% SDS-PAGE and transferred to polyvinylidene difluoride membranes.

After incubation in Odyssey blocking buffer (LI-COR Biosciences, Lincoln, NE) for 1 h, the membranes were probed with either 1:500 diluted anti-UGT1A9 antibody, 1:200 diluted anti-HNF1α antibody, or 1:200 diluted anti-β-actin antibody for 3 h followed by incubation with the corresponding fluorescent dye-conjugated secondary antibodies. The UGT1A9 or HNF1α protein levels in individual human liver samples were normalized with β-actin protein levels. The band densities were quantified with the Odyssey Infrared Imaging system (LI-COR Biosciences).

Propofol *O*-Glucuronosyltransferase Activity. The activity was determined as described previously (Fujiwara et al., 2007) with a substrate concentration of 500 μM.

Statistical Analyses. Correlation analyses were performed by the Pearson product-moment method. Differences between groups were determined by analysis of variance followed by the Tukey multiple comparison test. $p < 0.05$ was considered statistically significant.

Results

Selection of a Peptide Antigen to Generate UGT1A9 Antibody. Initially, preparation of a mouse monoclonal antibody against UGT1A9 was attempted using a histidine-tagged full-length UGT1A9 protein as an antigen. However, all of the resulting antibody clones (30 clones) cross-reacted with other UGT1A isoforms (data not shown). The full-length amino acid sequence of UGT1A9 exhibits homology with UGT1A7, UGT1A8, and UGT1A10 in excess of 88% (Table 1). Therefore, we next sought to prepare the monoclonal antibody using a UGT1A9 peptide as an antigen. Although peptides ranging from 10 to 20 amino acid residues in length are generally used for antigens, we used a relatively longer peptide, expecting that it could recognize three-dimensional structure. Residues 87 to 118 of UGT1A9 (32 amino acids) were selected as an antigen; this peptide sequence is contained within the longer peptide antigen (82 amino acids, residues 61–142) used by Girard et al. (2004) (Table 1). The amino acid homology of the two different antigenic peptides with the corresponding residues of UGT1A7, UGT1A8, and UGT1A10 was 59 to 63% (32-residue peptide) versus 80% (82-residue peptide). Thus, the peptide comprising the 87 to 118 amino acid residues of UGT1A9 was used as an antigen.

Specificity of the Prepared Antibody against UGT1A9. The specificity of the 40 candidate antibody clones was evaluated by

DRUG METABOLISM AND DISPOSITION DMD aspet

TABLE 1

Sequence alignment around the candidate peptide of UGT1A9 as an antigen with the other UGT1As

Multiple sequence alignment was performed using the ClustalW2 program (http://www.ebi.ac.uk/Tools/msa/clustalw2/) for amino acid residues 61 to 142 of UGT1A9, which were used as an antigen by Girard et al. (2004). Amino acids that are identical with those of UGT1A9 are in bold type. The peptide comprising amino acid residues 87 to 118 that was used as antigen in this study is in italic type.

Isoform	Accession No.	Sequence	Identity with UGT1A9 (%)		
			87–118	61–142	Full-Length
UGT1A1	P22309	$_{63}$**DASLYIRDGAFYTLKTYPVPFPQREDVKESFVSLGHNVFE**--NDSPLQRVIKTYKKIKKDSAMLLSGCSHLLHNKELMASLAESSF$_{145}$	12	24	66
UGT1A3	P35503	$_{64}$**EVAMHIKEENFFTLTTYAISWTQDEFDRHVLGHTQLYPE**--TEHFLKKFFRSMAMLNNMSLVYHRSCVELLHNEALIRHLNATSF$_{146}$	9	20	67
UGT1A4	P22310	$_{64}$**EVAMHIKEEKFFTLTAYAVPWTQKEFDRVTLGYTQGFPE**--TEHLLKRYSRSMAIMNNVSLALHRCCVELLHNEALIRHLNATSF$_{146}$	9	17	67
UGT1A5	P35504	$_{64}$**EVAMYIKEENFFTLTTYAISWTQDEFDRLLLGHTQSFPE**--TEHLLMKFSRRMAIMNNMSLIIHRSCVELLHNEALIRHLHATSF$_{146}$	6	18	67
UGT1A6	P19224	$_{62}$**EVNLLLKESKYYTKIYPVPYDQEELKNRYQSFGNNHF**--AERSFLTAPQTEYRNNMIVIGLYFINCQSLLQDRDTLNFFKESKF$_{144}$	12	29	68
UGT1A7	NP_061950	$_{61}$**EVSWQLGRSLNCTVKTYSTSTYTLEDQDREFMVFADARWTAPLRSAFSLLTSSSNG---IFDLFFSNCRSLFNDRKLVEYLKESCF**$_{142}$	59	80	93
UGT1A8	AAB8425	$_{61}$**EVSWQLGKSLNCTVKTYSTSTYTLEDLDREFMDFADAQWKAQVRSLFSLSSSNG---FFNLFFSHCRSLFNDRRLVEYLKESSF**$_{142}$	63	80	94
UGT1A9	NP_066307	$_{61}$**EVSWQLGRSLNCTVKTYSTSTYTLEDLDREFKAFAHAQWKAQVRSIYSLLMGSYND---IFDLFFSNCRSLFKDKKLVEYLKESSF**$_{142}$			
UGT1A10	AAB81537	$_{61}$**EVSWQLERSLNCTVKTYSTSTYTLED**QNREFMVFAHAQWKAQAQSIFSLLMSSSSG---FLDLFFSHCRSLFNDRKLVEYLKESSF$_{143}$	63	80	88

Western blot analysis using a panel of recombinant human UGT1A isoforms. Of the 40 clones, 5 reacted with UGT1A9 without cross-reacting with the other UGT1A isoforms (data not shown), from which the clone exhibiting the highest reactivity was selected for expansion and antibody production. The specificity of the purified antibody was then confirmed (Fig. 1A). Next, we investigated whether the antibody reacted with UGTs in human, mouse, and rat liver microsomes (Fig. 1B). The mouse Ugt1a9, Ugt1a7c, and Ugt1a10 exhibit 77 to 78% amino acid sequence homology with human UGT1A9 (Table 2). In rat, the *Ugt1a9* gene is a pseudogene, whereas Ugt1a7, Ugt1a8, and Ugt1a10, which are functional proteins, exhibit 76 to 79% amino acid homology with human UGT1A9. As shown in Fig. 1B, a clear single band was observed only with human liver microsomes, suggesting that the antibody does not react with any Ugt in mouse and rat livers.

Reactivity of the Antibody toward Glycosylated or Deglycosylated UGT1A9. We previously reported that UGT1A9 is glycosylated at three asparagine residues at position 71, 292, and 344 (Nakajima et al., 2010). Three bands observed in UGT1A9 Supersomes (Fig. 1A) would represent differently glycosylated species of UGT1A9, because none of them were observed in the other UGT1A Supersomes. We investigated whether the antibody could recognize both glycosylated and deglycosylated or unglycosylated UGT1A9. When the UGT1A9 Supersomes were treated with Endo H, the upper two bands observed in the nontreated sample disappeared, and a band with higher mobility was observed. The density of the faster migrating band appeared higher than that of the sum of the upper two bands (Fig. 1C, left). The fastest migrating band in the nontreated sample might be the glycosylated form that is tolerable to Endo H or other post-translationally modified form. The recombinant UGT1A9 stably expressed in HEK293 cells also showed three bands (Fig. 1C, left), but the upper two bands would be nonspecific bands because they were observed in homogenates from mock HEK293 cells too (data not shown). The difference in the band patterns between UGT1A9 Supersomes and UGT1A9 in HEK293 cells might reflect the differences in the extent of glycosylation and/or size of the glycan in insect or mammalian cells. When the recombinant UGT1A9 in HEK293 cells was treated with Endo H, the fastest migrating band was clearly shifted (Fig. 1C, left). The band density was higher than that in the nontreated sample. As for HLM, the mobility of UGT1A9 was similar to that of UGT1A9 expressed in HEK293 cells, and UGT1A9 in HLM appeared to show some tolerance to Endo H. Next, we used PNGase F, which can cleave Endo H-resistant *N*-glycans (probably *N*-glycans from which two mannose subunits are removed by Golgi α-mannosidase II). By the treatment of HLM with PNGase F, only a band with faster mobility was observed, indicating that the upper band observed in Endo H-treated HLM would be the Endo H-resistant glycosylated UGT1A9 (Fig. 1C, right). In the cases of UGT1A9 Supersomes and UGT1A9 in HEK293 cells, the results with PNGase F treatment were the same as those with Endo H treatment. It is interesting that the deglycosylated UGT1A9 in UGT1A9 Supersomes and UGT1A9 in HEK293 cells and HLM differently migrated, although it is still unclear whether other post-translational modifications such as phosphorylation may be involved. Taken together, these results suggest that the antibody can recognize UGT1A9 regardless of glycosylation status, although the reactivity seems to be enhanced for unglycosylated UGT1A9.

UGT1A9 Protein Expression in Human Tissues. Previous studies reported that UGT1A9 mRNA is predominantly expressed in the liver and the kidney, and, to a much lesser extent, in adrenal, colon, small intestine, esophagus, testis, and bladder tissues (Nakamura et al., 2008; Ohno and Nakajin, 2009). We obtained microsomes from human liver, kidney, jejunum, and ileum, which we subjected to

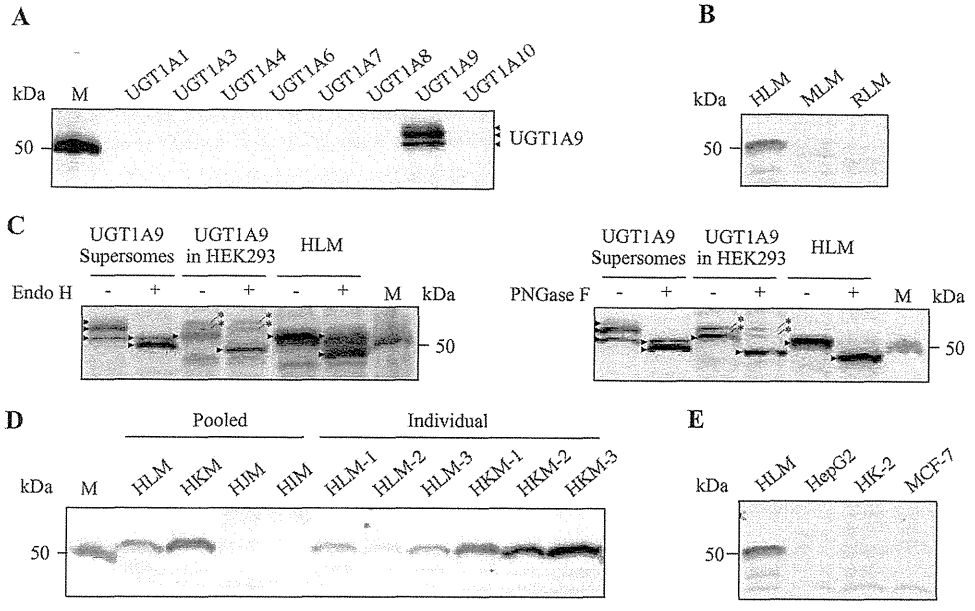

FIG. 1. Western blot analyses using the monoclonal antibody against human UGT1A9. A, recombinant UGT1As (10 μg) expressed in baculovirus-infected insect cells (Supersomes). B, pooled microsomes from human, mouse, or rat liver (30 μg). C, Endo H-treated (left) or PNGase F-treated (right) (+) and nontreated (−) UGT1A9 Supersomes (2.5 μg), recombinant UGT1A9 stably expressed in HEK293 (40 μg), and HLM (30 μg). D, microsomes from human liver, kidney, jejunum, and ileum (15 μg). E, microsomes from human liver and human cell lines (30 μg). In C, the arrowhead and asterisk represent UGT1A9 and the nonspecific band, respectively. MLM, mouse liver microsomes; RLM, rat liver microsomes; HKM, human kidney microsomes; HJM, human jejunum microsomes; HIM, human ileum microsomes; M, marker.

TABLE 2

Sequence alignment of the candidate peptide of human UGT1A9 as an antigen with highly similar rodent Ugt1a isoforms

Multiple sequence alignment was performed using the ClustalW2 program (http://www.ebi.ac.uk/Tools/msa/clustalw2/) for amino acid residues 87 to 118 and those of the corresponding region of rodent Ugt1a isoforms. Amino acids that are identical with those of UGT1A9 are in bold type.

Isoform	Accession No.	Sequence	Identity with UGT1A9 (%)	
			87–118	Full-Length
Human UGT1A9	NP_066307	$_{87}$**DREFKAFAHAQWKAQVRS-IYSLLMGSYNDIFD**$_{118}$		
Mouse Ugt1a7c	AAP48598	$_{87}$**NREFK**ISID**AQWKS**QQEGGI**LPLL**DSPAKGF**FE**$_{119}$	40	77
Mouse Ugt1a9	AAP48599	$_{85}$**DREFK**YLSYT**QWKT**PEH**S**-**IRSFLTGS**ARGF**FE**$_{116}$	47	78
Mouse Ugt1a10	AAP48600	$_{87}$**DREFKYF**TYT**QWKT**PEQ**S**-**IRSFMTGS**ARGF**FE**$_{118}$	47	78
Rat Ugt1a7	AAR95635	$_{87}$**NREFKFF**IDS**QWKT**QQEGGVL**PLL**TSPAQGF**FE**$_{119}$	36	77
Rat Ugt1a8	AAR95636	$_{87}$NYH**FKFFAH**NQ**WKT**QEVG-MF**SLL**KHS**G**KGF**FE**$_{118}$	44	79
Rat Ugt1a10	AAR95630	$_{87}$**DREFKH**F**S**YT**QWKT**PEQ**S**-M**YSL**IT**GS**VK**D**FLE$_{118}$	50	76

Western blot analysis. As shown in Fig. 1D, high expression of UGT1A9 protein was detected in the kidney, followed by the liver, but negligible expression was observed in the jejunum and the ileum, consistent with the previously reported mRNA expression profiles. To investigate whether UGT1A9 expression is generally higher in the kidney than in the liver, liver and kidney microsomes obtained from three individuals were subjected to Western blot analysis. We found that the relative UGT1A9 protein levels are approximately 3 to 16 times higher in the kidney than in the liver.

UGT1A9 Protein Expression in Human Cell Lines. We previously reported that UGT1A9 is detectable at the mRNA level in human cell lines, including HepG2, HK-2, and MCF-7 (Nakamura et al., 2008), for which reproducibility was confirmed by quantitative real-time reverse transcriptase-polymerase chain reaction (data not shown). However, to date, there has been no reported quantitation of UGT1A9 at the protein level in human cell lines using an isoform-specific antibody. We investigated whether UGT1A9 protein could be detected in HepG2, HK-2, and MCF-7 cell lines using the antibody that we generated. When the microsomes from these cell lines were subjected to Western blot analysis, no band was observed, which is probably attributed to low UGT1A9 expression levels in these cells (Fig. 1E).

Normalized Activities of UGT1A9 in Recombinant Systems and Human Tissue Microsomes. The prepared specific antibody against UGT1A9 enabled us to determine the normalized activities per unit of UGT1A9 in recombinant systems and human tissue microsomes. We determined the relative expression levels of UGT1A9 protein in UGT1A9 Supersomes and recombinant UGT1A9 stably expressed in HEK293 cells, HLM, and human kidney microsomes as 59 ± 7.7, 1.0 ± 0.0, 5.6 ± 0.8, and 11.6 ± 0.7 units/μg protein, respectively (Fig. 2A). The propofol O-glucuronidation activities in these enzyme sources were 4598 ± 309, 400 ± 98, 3275 ± 99, and 6418 ± 635 pmol · min^{-1} · mg $protein^{-1}$, respectively (Fig. 2B). Accordingly, it was demonstrated that the normalized activities per unit of UGT1A9 in UGT1A9 Supersomes and recombinant UGT1A9 in HEK293 cells were 7- and 1.4-fold, respectively, lower than those in human tissue microsomes (Fig. 2C).

Expression Levels of UGT1A9 Protein in Individual Human Livers and the Correlation of Protein with mRNA Levels and Enzymatic Activity. We assessed the relative expression levels of UGT1A9 protein in a panel of 20 human liver microsomes and found a 9-fold interindividual variability (Fig. 3A). The UGT1A9 protein level normalized with β-actin seems to be higher in Japanese than in other ethnic groups. However, it may be due to a lower β-actin level in Japanese than in the other ethnic groups. To draw a definitive conclusion for the ethnic difference, analysis with a larger sample size is necessary. The UGT1A9 protein levels were moderately correlated ($r = 0.48$, $p < 0.05$) with propofol *O*-glucuronosyltransferase activity (Fig. 3B). However, the UGT1A9 protein levels were not correlated ($r = -0.13$) with the UGT1A9 mRNA levels that were determined in

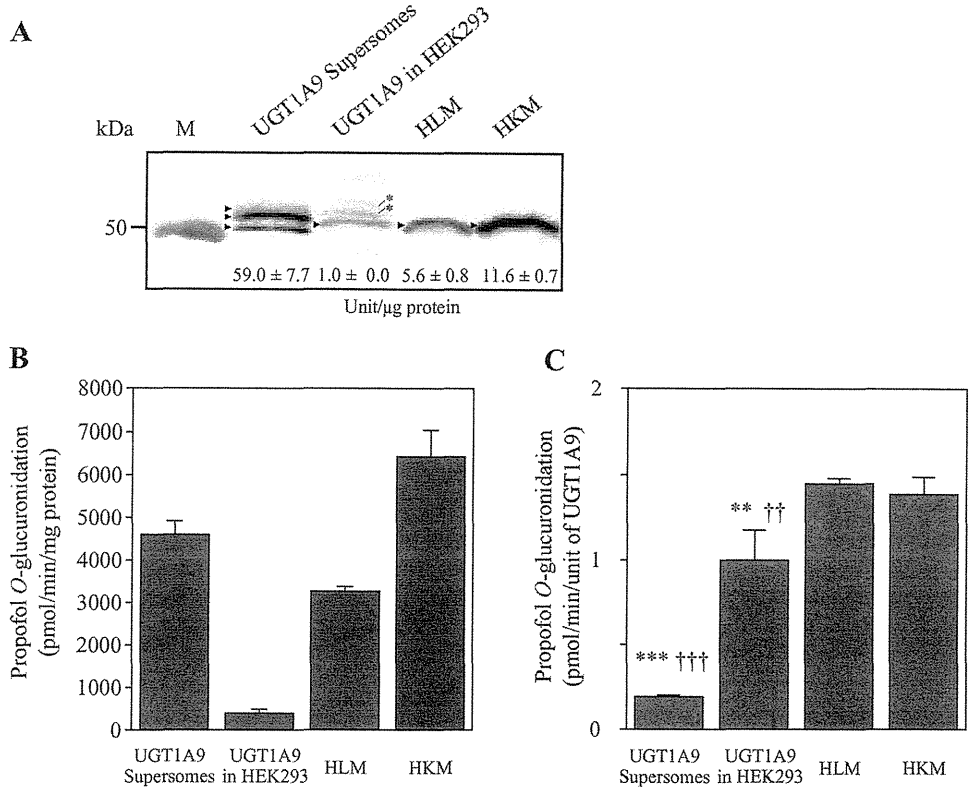

FIG. 2. UGT1A9 protein expression and propofol O-glucuronidation in recombinant UGT1A9 expression systems and human tissue microsomes. A, Western blot analysis of UGT1A9 protein in UGT1A9 Supersomes (2.5 μg) and recombinant UGT1A9 stably expressed in HEK293 (40 μg), HLM (15 μg), and human kidney microsomes (HKM) (15 μg). The values shown in the membrane indicate the expression level of UGT1A9 expressed as units of UGT1A9 per microgram of protein. Data are the means ± S.D. of quadruplicate determinations. The arrowhead and asterisk represent UGT1A9 and the nonspecific band, respectively. B and C, propofol O-glucuronidation activity in these enzyme sources expressed as picomoles per minute per milligram of protein (B) and picomoles per minute per unit of UGT1A9 protein (C). Columns represent the means ± S.D. of triplicate determinations. **, $p < 0.01$; ***, $p < 0.001$, compared with HLM; ††, $p < 0.01$; †††, $p < 0.001$, compared with HKM. M, marker.

our previous study (Fig. 3C), exhibiting a 150-fold variability (Izukawa et al., 2009). Previous studies (Aueviriyavit et al., 2007; Ramírez et al., 2008) reported that HNF1α and HNF4α mRNA levels were strongly correlated with UGT1A9 mRNA levels in a panel of human livers, which is consistent with the finding that HNF1α and HNF4α contribute to the regulation of UGT1A9 (Barbier et al., 2005; Gardner-Stephen and Mackenzie, 2007). However, the HNF protein levels rather than mRNA level should be considered. Thus, we investigated whether the HNF1α and HNF4α protein levels are correlated with the UGT1A9 mRNA or protein levels. We found that the HNF1α protein levels were significantly correlated with the UGT1A9 mRNA levels ($r = 0.52$, $p < 0.05$) but not with the UGT1A9 protein levels ($r = -0.24$, not significant) (Fig. 3, D and E). These data suggest that whereas HNF1α may regulate UGT1A9 at the transcriptional level, UGT1A9 protein levels are being regulated at the post-transcriptional level. Unfortunately, we could not assess the HNF4α protein levels because of an insufficient dynamic range of the antibody used (data not shown).

Discussion

Human UGT1A9 is one of the physiologically and pharmacologically important UGT1A isoforms, metabolizing a wide spectrum of substrates including bulky phenols, dietary constituents, steroids, and fatty acids, as well as currently prescribed drugs including anticancer agents, fibrates, nonsteroidal anti-inflammatory drugs and antiarrhythmic agents (Ritter, 2000). Human UGT1A9 mRNA was found to be predominantly expressed in liver and kidney and to a lesser extent in esophagus, small intestine, colon, adrenal gland, and bladder (Nakamura et al., 2008; Ohno and Nakajin, 2009). However, further information regarding UGT1A9 protein has been limited by the lack of a specific antibody against UGT1A9. Although there were previous attempts to generate specific antibodies against UGT1A9 (Girard et al., 2004; Ikushiro et al., 2006), the antibodies recognized other UGT1A isoforms such as UGT1A6 (Ikushiro et al., 2006), UGT1A7, UGT1A8, and UGT1A10 (Girard et al., 2004). Furthermore, when we evaluated the specificity of commercially available antibodies against UGT1A9 (Abcam, Cambridge, UK; Abnova, Taipei, Taiwan), we observed that these antibodies cross-reacted with other UGT1A isoforms (S. Oda and M. Nakajima, unpublished data). This background prompted us to prepare a specific antibody against human UGT1A9. We used a peptide containing the amino acid residues 87 to 118 of UGT1A9 as an antigen. Although this peptide is relatively longer than those generally used as antigens, it is shorter than the peptide antigen used by Girard et al. (2004) that contained UGT1A9 amino acid residues 61 to 142. Here, we report the first successful generation of an antibody that specifically recognizes UGT1A9.

Upon Western blotting using the prepared antibody, we confirmed that there was no aggregated UGT1A9 at the interface between the upper and lower gels or the bottom of the wells in any enzyme source (data not shown). The expression level of UGT1A9 protein was found to be highest in the kidney, followed by the liver, but was negligible in jejunum and ileum (Fig. 1D), consistent with previously reported mRNA data (Nakamura et al., 2008; Ohno and Nakajin, 2009). Although the kidney plays a role in the excretion of polar xenobiotics and metabolites, increasing evidence reveals that the kidney significantly contributes to metabolic clearance of therapeutic drugs, such as nonsteroidal anti-inflammatory drugs, propofol, and mycophenolic acid, and to the maintenance of renal homeostasis through inactivating mediators, such as prostaglandins, leukotrienes, epoxyeicosatrienoic acids, and hydroxyeicosatetraenoic acids (Knights and Miners, 2010). Because these drugs or endobiotics are known to be substrates of UGT1A9 (Knights and Miners, 2010), it has been speculated that UGT1A9 would contribute to their clearance. There has been only one report of the immunohistochemical detection of UGT1A (Gaganis et al., 2007), although the precise isoforms detected remain unknown. The present study supports the role of UGT1A9 in the kidney, as

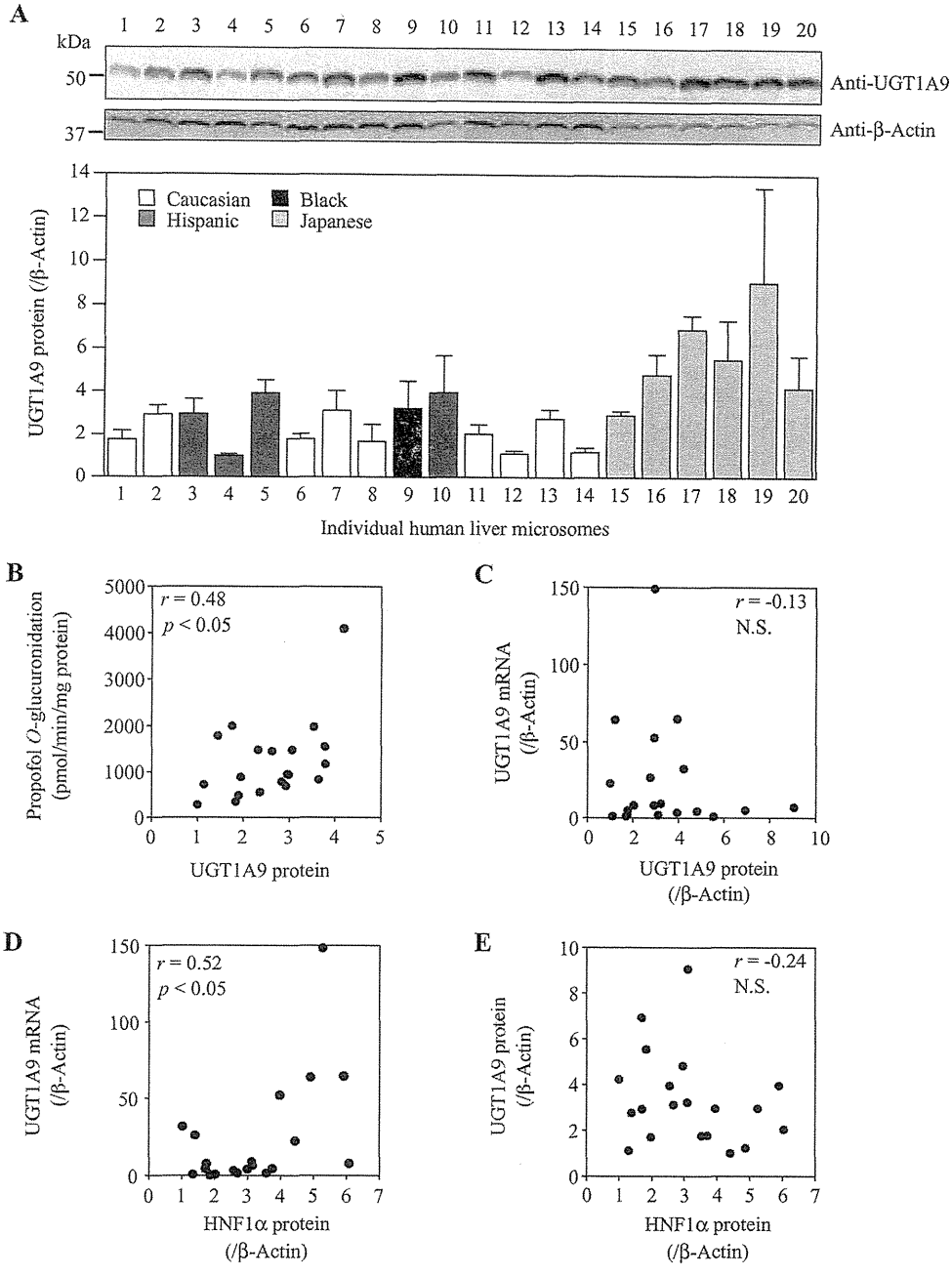

FIG. 3. Interindividual variability of UGT1A9 protein levels in human liver and its correlation with enzyme activity, UGT1A9 mRNA, or HNF1α protein levels. A, expression levels of UGT1A9 protein in 20 human liver microsomes were determined by Western blot analysis. Data are the means ± S.D. of triplicate determinations. Relationships between UGT1A9 protein levels and propofol *O*-glucuronosyltransferase activities (B), between UGT1A9 protein levels and UGT1A9 mRNA levels (C), between HNF1α protein levels and UGT1A9 mRNA levels (D), and between HNF1α protein levels and UGT1A9 protein levels (E) were analyzed. The propofol *O*-glucuronosyltransferase activity was measured at a substrate concentration of 500 μM. The UGT1A9 mRNA levels were normalized to β-actin mRNA levels. The UGT1A9 and HNF1α protein levels were normalized to β-actin protein levels. The values represent the levels relative to that of the lowest sample. Each data point is the mean of duplicate experiments except UGT1A9 protein level. N.S., not significant.

indicated by the substantial expression of UGT1A9 protein detected by Western blotting. The antibody that we prepared will be useful for future immunohistochemical studies of UGT1A9.

An interesting finding using the prepared antibody was that the normalized activities of UGT1A9 in recombinant systems were unambiguously lower than those in human tissue microsomes (Fig. 2). This might be attributable to the differences in membrane circumstance including lipid components and/or post-translational modification between recombinant systems and human tissue microsomes. Another possible explanation is the presence of other UGT isoforms in human tissue microsomes. Previous studies (Fujiwara et al., 2007, 2010) demonstrated that the coexpression of another UGT isoform increases the UGT1A9-catalyzed propofol *O*-glucuronidation in HEK293 cells. Apart from these reasons, it is notable that the activities of recombinant UGTs do not directly and quantitatively mirror the actual UGT activities in human tissues. In this regard, the relative activity factor approach (Crespi and Miller, 1999), which uses the ratio of activity of tissue microsomes and recombinant enzymes, would be useful to estimate the contributions of individual UGTs to a given metabolic pathway in tissue microsomes, as recent studies reported (Kato et al., 2012; Zhu et al., 2012).

We found moderate interindividual variability (9-fold) of hepatic UGT1A9 expression at the protein level (Fig. 3). Several studies have sought to uncover the underlying mechanisms of the variability in the UGT1A9 expression, with particular focus on *cis*- or *trans*-acting factors. As *cis*-acting factors, genetic polymorphisms can be raised. The *−275 T>A* and *−2152 C>T* alleles, which are linked to each other, have been shown to be associated with higher hepatic UGT1A9 protein expression and increased rates of propofol and mycophenolic acid glucuronidation (Girard et al., 2004). In addition, homozygotes

for the intronic single nucleotide polymorphism at position *IVS1 +399C>T* have been shown to exhibit higher (1.3-fold) hepatic UGT1A9 protein levels (Girard et al., 2006). In these studies, UGT1A9 protein was assessed using the UGT1A7–10 antibody. The fact that UGT1A7, UGT1A8, and UGT1A10 are not expressed in liver made such studies possible. In contrast, our antibody would be applicable for the evaluation of the effects of this single nucleotide polymorphism on UGT1A9 expression in extrahepatic tissues expressing UGT1A9 and the closely related isoforms UGT1A7, UGT1A8, and UGT1A10, such as kidney and adrenal tissues (Ohno and Nakajin, 2009). As *trans*-acting factors, transcription factors can be raised. It has been reported that HNF1α and HNF4α positively regulate the expression of UGT1A9 (Barbier et al., 2005; Gardner-Stephen and Mackenzie, 2007). A significant positive correlation between these factors and UGT1A9 at the mRNA level in human livers has been reported (Aueviriyavit et al., 2007; Ramírez et al., 2008). Beyond these reports, we demonstrated that HNF1α protein levels are significantly correlated with UGT1A9 mRNA levels (Fig. 3D). However, HNF1α protein levels were not correlated with UGT1A9 protein levels (Fig. 3E), because we did not detect any correlation between the UGT1A9 mRNA and protein levels (Fig. 3C). Lack of correlation between the mRNA and protein levels has also been observed with other UGTs, such as UGT1A4, UGT1A6, and UGT2B7 (Izukawa et al., 2009). Therefore, it is reasonable to speculate that post-transcriptional and/or post-translational regulation plays a role in UGT protein levels. MicroRNAs (miRNAs) have recently received considerable attention as a critical factor of post-transcriptional regulation. We have reported that some cytochrome P450 isoforms and transcriptional factors, such as pregnane X receptor, vitamin D receptor, and HNF4α are regulated by miRNAs (Nakajima and Yokoi, 2011), implying that miRNAs have a role in clearance of drugs and endobiotics. It would be of interest to investigate whether miRNAs may be involved in the regulation of UGTs. In general, mammalian miRNAs bind to the 3′-untranslated region of the target mRNA to cause translational repression or mRNA degradation. Because the 3′-untranslated sequences of UGT1As are common, it is possible that UGT1As may be commonly regulated by the same miRNA.

The UGT1A9 protein levels in a panel of 20 individual human livers were moderately ($r = 0.48$, $p < 0.05$) correlated with propofol glucuronidation (Fig. 2B). The moderate correlation was consistent ($r = 0.5$, $p < 0.0001$, $n = 48$) with the results reported by Girard et al. (2004). Because we previously demonstrated that UGT enzyme activity could be modulated through formation of heterodimers with other UGT isoform (Fujiwara et al., 2007), such modulation might account for the moderate correlation.

In summary, we generated a specific monoclonal antibody against human UGT1A9. By Western blot analysis using this antibody, we found that human UGT1A9 protein is highly expressed in the kidney and the liver but not in the jejunum or the ileum, supporting previous findings at mRNA levels. This antibody can be used to assess tissue distribution and interindividual variability of UGT1A9 protein expression, and such evaluation may promote the understanding of the physiological, pharmacological, and toxicological role of UGT1A9.

Acknowledgments

We acknowledge Drs. Yasuhiro Aoki and Masataka Takamiya at Iwate Medical University for supplying human livers.

Authorship Contributions

Participated in research design: Oda, Nakajima, Hatakeyama, Fukami, and Yokoi.

Conducted experiments: Oda.

Contributed new reagents or analytic tools: Hatakeyama.

Performed data analysis: Oda.

Wrote or contributed to the writing of the manuscript: Oda, Nakajima, and Yokoi.

References

Aueviriyavit S, Furihata T, Morimoto K, Kobayashi K, and Chiba K (2007) Hepatocyte nuclear factor 1α and 4α are factors involved in interindividual variability in the expression of UGT1A6 and UGT1A9 but not UGT1A1, UGT1A3 and UGT1A4 mRNA in human livers. *Drug Metab Pharmacokinet* **22:**391–398.

Barbier O, Girard H, Inoue Y, Duez H, Villeneuve L, Kamiya A, Fruchart JC, Guillemette C, Gonzalez FJ, and Staels B (2005) Hepatic expression of the *UGT1A9* gene is governed by hepatocyte nuclear factor 4α. *Mol Pharmacol* **67:**241–249.

Chou PY and Fasman GD (1974) Prediction of protein conformation. *Biochemistry* **13:**222–245.

Crespi CL and Miller VP (1999) The use of heterologously expressed drug metabolizing enzymes—state of the art and prospects for the future. *Pharmacol Ther* **84:**121–131.

Emini EA, Hughes JV, Perlow DS, and Boger J (1985) Induction of hepatitis A virus: neutralizing antibody by a virus-specific synthetic peptide. *J Virol* **55:**836–839.

Formelli F, Barua AB, and Olson JA (1996) Bioactivities of *N*-(4-hydroxyphenyl) retinamide and retinoyl β-glucuronide. *FASEB J* **10:**1014–1024.

Fujiwara R, Nakajima M, Oda S, Yamanaka H, Ikushiro S, Sakaki T, and Yokoi T (2010) Interactions between human UDP-glucuronosyltransferase (UGT) 2B7 and UGT1A enzymes. *J Pharm Sci* **99:**442–454.

Fujiwara R, Nakajima M, Yamanaka H, Nakamura A, Katoh M, Ikushiro S, Sakaki T, and Yokoi T (2007) Effects of coexpression of UGT1A9 on enzymatic activities of human UGT1A isoforms. *Drug Metab Dispos* **35:**747–757.

Gaganis P, Miners JO, Brennan JS, Thomas A, and Knights KM (2007) Human renal cortical and medullary UDP-glucuronosyltransferases (UGTs): immunohistochemical localization of UGT2B7 and UGT1A enzymes and kinetic characterization of *S*-naproxen glucuronidation. *J Pharmacol Exp Ther* **323:**422–430.

Gardner-Stephen DA and Mackenzie PI (2007) Hepatocyte nuclear factor1 transcription factors are essential for the UDP-glucuronosyltransferase 1A9 promoter response to hepatocyte nuclear factor 4α. *Pharmacogenet Genomics* **17:**25–36.

Garnier J, Osguthorpe DJ, and Robson B (1978) Analysis of the accuracy and implications of simple methods for predicting the secondary structure of globular proteins. *J Mol Biol* **120:**97–120.

Girard H, Court MH, Bernard O, Fortier LC, Villeneuve L, Hao Q, Greenblatt DJ, von Moltke LL, Perussed L, and Guillemette C (2004) Identification of common polymorphisms in the promoter of the UGT1A9 gene: evidence that UGT1A9 protein and activity levels are strongly genetically controlled in the liver. *Pharmacogenetics* **14:**501–515.

Girard H, Villeneuve L, Court MH, Fortier LC, Caron P, Hao Q, von Moltke LL, Greenblatt DJ, and Guillemette C (2006) The novel UGT1A9 intronic I399 polymorphism appears as a predictor of 7-ethyl-10-hydroxycamptothecin glucuronidation levels in the liver. *Drug Metab Dispos* **34:**1220–1228.

Gong QH, Cho JW, Huang T, Potter C, Gholami N, Basu NK, Kubota S, Carvalho S, Pennington MW, Owens IS, et al. (2001) Thirteen UDP-glucuronosyltransferase genes are encoded at the human *UGT1* gene complex locus. *Pharmacogenetics* **11:**357–368.

Guillemette C (2003) Pharmacogenomics of human UDP-glucuronosyltransferase enzymes. *Pharmacogenomics J* **3:**136–158.

Hopp TP and Woods KR (1981) Prediction of protein antigenic determinants from amino acid sequences. *Proc Natl Acad Sci USA* **78:**3824–3828.

Ikushiro S, Emi Y, Kato Y, Yamada S, and Sakaki T (2006) Monospecific antipeptide antibodies against human hepatic UDP-glucuronosyltransferase 1A subfamily (UGT1A) isoforms. *Drug Metab Pharmacokinet* **21:**70–74.

Izukawa T, Nakajima M, Fujiwara R, Yamanaka H, Fukami T, Takamiya M, Aoki Y, Ikushiro S, Sakaki T, and Yokoi T (2009) Quantitative analysis of UDP-glucuronosyltransferase (UGT) 1A and UGT2B expression levels in human livers. *Drug Metab Dispos* **37:**1759–1768.

Kato Y, Nakajima M, Oda S, Fukami T, and Yokoi T (2012) Human UDP-glucuronosyltransferase isoforms involved in haloperidol glucuronidation and quantitative estimation of their contribution. *Drug Metab Dispos* **40:**240–248.

Knights KM and Miners JO (2010) Renal UDP-glucuronosyltransferases and the glucuronidation of xenobiotics and endogenous mediators. *Drug Metab Rev* **42:**63–73.

Mackenzie PI, Gregory PA, Gardner-Stephen DA, Lewinsky RH, Jorgensen BR, Nishiyama T, Xie W, and Radominska-Pandya A (2003) Regulation of UDP glucuronosyltransferase genes. *Curr Drug Metab* **4:**249–257.

Mackenzie PI, Bock KW, Burchell B, Guillemette C, Ikushiro S, Iyanagi T, Miners JO, Owens IS, and Nebert DW (2005) Nomenclature update for the mammalian UDP glycosyltransferase (*UGT*) gene superfamily. *Pharmacogenet Genomics* **15:**677–685.

Nakajima M, Koga T, Sakai H, Yamanaka H, Fujiwara R, and Yokoi T (2010) *N*-Glycosylation plays a role in protein folding of human UGT1A9. *Biochem Pharmacol* **79:**1165–1172.

Nakajima M and Yokoi T (2011) MicroRNAs from biology to future pharmacotherapy: regulation of cytochrome P450s and nuclear receptors. *Pharmacol Ther* **131:**330–337.

Nakamura A, Nakajima M, Yamanaka H, Fujiwara R, and Yokoi T (2008) Expression of UGT1A and UGT2B mRNA in human normal tissues and various cell lines. *Drug Metab Dispos* **36:**1461–1464.

Ohno S and Nakajin S (2009) Determination of mRNA expression of human UDP-glucuronosyltransferases and application for localization in various human tissues by real-time reverse transcriptase-polymerase chain reaction. *Drug Metab Dispos* **37:**32–40.

Ohtsuki S, Schaefer O, Kawakami H, Inoue T, Liehner S, Saito A, Ishiguro N, Kishimoto W, Ludwig-Schwellinger E, Ebner T, et al. (2012) Simultaneous absolute protein quantification of transporters, cytochromes P450, and UDP-glucuronosyltransferases as a novel approach for the characterization of individual human liver: comparison with mRNA levels and activities. *Drug Metab Dispos* **40:**83–92.

Parker JM, Guo D, and Hodges RS (1986) New hydrophilicity scale derived from high-performance liquid chromatography peptide retention data: correlation of predicted surface residues with antigenicity and X-ray-derived accessible sites. *Biochemistry* **25:**5425–5432.

Ramírez J, Mirkov S, Zhang W, Chen P, Das S, Liu W, Ratain MJ, and Innocenti F (2008)

Hepatocyte nuclear factor-1α is associated with *UGT1A1*, *UGT1A9* and *UGT2B7* mRNA expression in human liver. *Pharmacogenomics J* **8:**152–161.
Ritter JK (2000) Roles of glucuronidation and UDP-glucuronosyltransferases in xenobiotic bioactivation reactions. *Chem Biol Interact* **129:**171–193.
Shimomura K, Kamata O, Ueki S, Ida S, and Oguri K (1971) Analgesic effect of morphine glucuronides. *Tohoku J Exp Med* **105:**45–52.
Strassburg CP, Kneip S, Topp J, Obermayer-Straub P, Barut A, Tukey RH, and Manns MP (2000) Polymorphic gene regulation and interindividual variation of UDP-glucuronosyltransferase activity in human small intestine. *J Biol Chem* **275:**36164–36171.
Strassburg CP, Oldhafer K, Manns MP, and Tukey RH (1997) Differential expression of the *UGT1A* locus in human liver, biliary, and gastric tissue: identification of *UGT1A7* and *UGT1A10* transcripts in extrahepatic tissue. *Mol Pharmacol* **52:**212–220.
Sutherland L, Ebner T, and Burchell B (1993) The expression of UDP-glucuronosyltransferases of the UGT1 family in human liver and kidney and in response to drugs. *Biochem Pharmacol* **45:**295–301.
Tabata T, Katoh M, Tokudome S, Hosakawa M, Chiba K, Nakajima M, and Yokoi T (2004) Bioactivation of capecitabine in human liver: involvement of the cytosolic enzyme on 5′-deoxy-5-fluorocytidine formation. *Drug Metab Dispos* **32:**762–767.
Welling GW, Weijer WJ, van der Zee R, and Welling-Wester S (1985) Prediction of sequential antigenic regions in proteins. *FEBS Lett* **188:**215–218.
Zhu L, Ge G, Zhang H, Liu H, He G, Liang S, Zhang Y, Fang Z, Dong P, Finel M, et al. (2012) Characterization of hepatic and intestinal glucuronidation of magnolol: application of the relative activity factor approach to decipher the contributions of multiple UDP-glucuronosyltransferase isoforms. *Drug Metab Dispos* **40:**529–538.

Address correspondence to: Dr. Miki Nakajima, Drug Metabolism and Toxicology, Faculty of Pharmaceutical Sciences, Kanazawa University, Kakuma-machi, Kanazawa 920-1192, Japan. E-mail: nmiki@p.kanazawa-u.ac.jp

Toxicology 293 (2012) 107–114

Contents lists available at SciVerse ScienceDirect

Toxicology

journal homepage: www.elsevier.com/locate/toxicol

Involvement of immune-related factors in diclofenac-induced acute liver injury in mice

Azusa Yano[a], Satonori Higuchi[a], Koichi Tsuneyama[b], Tatsuki Fukami[a], Miki Nakajima[a], Tsuyoshi Yokoi[a,*]

[a] Drug Metabolism and Toxicology, Faculty of Pharmaceutical Sciences, Kanazawa University, Kanazawa, Japan
[b] Department of Diagnostic Pathology, Graduate School of Medicine and Pharmaceutical Science for Research, University of Toyama, Japan

ARTICLE INFO

Article history:
Received 2 November 2011
Received in revised form
20 December 2011
Accepted 13 January 2012
Available online 25 January 2012

Keywords:
Diclofenac
Drug-induced liver injury
Inflammation
IL-1β
IL-17

ABSTRACT

Drug-induced liver injury (DILI) is a major safety concern in drug development and clinical drug therapy. However, the underlying mechanism of DILI is little known. It is difficult to predict DILI in humans due to the lack of experimental animal models. Diclofenac, a non-steroidal anti-inflammatory drug rarely causes severe liver injury in human, but there is some evidence for immunoallergic idiosyncratic reactions. In this study, the mechanism of diclofenac-induced liver injury in mice was investigated. First, we established the dosing condition for liver injury in normal mice. Plasma ALT and AST levels were significantly increased in diclofenac-administered (80 mg/kg, *i.p.*) mice in a dose- and time-dependent manner. Among several interleukins (ILs) and chemokines, mRNA expression of helper T (Th) 17 cell-mediated factors, such as retinoid orphan receptor (ROR)-γt, and signal transducers and activators of transcription factor (STAT) 3 in the liver, and the plasma IL-17 level were significantly increased. Neutralization of IL-17 tended to suppress the hepatotoxicity of diclofenac, suggesting that IL-17 was partly involved. Gadolinium chloride ($GdCl_3$) administration demonstrated that Kupffer cells are not likely to be involved in diclofenac hepatotoxicity. Hepatic expressions of IL-1β mRNA and plasma IL-1β were significantly increased soon after the diclofenac administration. Then, the results of an *in vivo* neutralization study of IL-1β suggested that IL-1β was involved early in the time of pathogenesis of the diclofenac-induced liver injury. In conclusion, we firstly developed a diclofenac-induced acute liver injury model in normal mice, and the involvement of IL-17 and IL-1β was clarified.

1. Introduction

Drug-induced liver injury (DILI) is the most frequent reason for the withdrawal of a drug from the market and cessation of new drug development in pharmaceutical companies. Due to their association with significant patient morbidity and mortality, several drugs have been removed from the pharmaceutical market, including bromfenac, ebrotidine, and troglitazone (Holt and Ju, 2006). In most cases, the mechanisms of the hepatotoxicity are unknown and predictive experimental animal models are still lacking.

Diclofenac, a nonsteroidal anti-inflammatory drug, causes an asymptomatic increase of plasma transaminase in approximately 15% of patients, and life-threatening fluminant hepatitis is induced in a very small percentage of patients (Bhogaraju et al., 1999). The molecular mechanisms of liver injury are largely unknown, but the involvement of a toxic metabolite has been suggested (Purcell et al., 1991). Diclofenac is metabolized to oxidative metabolites catalyzed by CYP2C9 and CYP3A4 (Tang et al., 1999), and these metabolites have the potential to be further oxidized to quinoneimine intermediates, which might be involved in the hepatocellular stress caused by diclofenac. On the other hand, there is clinical and experimental evidence that, in some cases, immune-related reactions are involved in diclofenac-induced liver injury, and the histopathological picture suggests hypersensitivity reactions (Boelsterli, 2003). Furthermore, one study reported that pretreatment of lipopolysaccharide (LPS) exacerbates diclofenac-hepatotoxicity in rats (Deng et al., 2006), suggesting that diclofenac-induced liver injury involves immune responses. However, as of now, the involvement of immune reactions underlying the severe liver injury induced by diclofenac remains to be clarified.

Helper T (Th) cell-mediated immune responses play pivotal roles in the pathogenesis of a variety of human liver disorders (Kita et al., 2001). The action of Th cells in the liver is mediated through the release of a variety of cytokines, which target liver cells and/or immune cells by activating multiple signaling cascades, including the signal transducers and activators of transcription factor

* Corresponding author at: Drug Metabolism and Toxicology, Faculty of Pharmaceutical Sciences, Kanazawa University, Kakuma-machi, Kanazawa 920-1192, Japan. Tel.: +81 76 234 4407; fax: +81 76 234 4407.
E-mail address: tyokoi@kenroku.kanazawa-u.ac.jp (T. Yokoi).

0300-483X/$ – see front matter © 2012 Elsevier Ireland Ltd. All rights reserved.
doi:10.1016/j.tox.2012.01.008

(STAT) family members (Leonard and O'Shea, 1998). Th cells are subdivided into Th1, Th2, and Th17 subsets by their unique production of cytokines and characteristic transcription factors. Th1 cells require "T-box expressed in T cells" (T-bet) and secrete interferon (IFN)-γ. Th2 cells require GATA-binding domain (GATA)-3 and produce interleukin (IL)-4 and IL-5. Retinoid-related orphan receptor (ROR)-γt is indispensable for the differentiation of Th17 cells, which mainly secret IL-17 (Kidd, 2003; Steinman, 2007; McGeachy and Cua, 2008). We previously reported that IL-17 is involved in halothane (Kobayashi et al., 2009) and α-naphthylisothiocyanate (ANIT)-induced liver injury (Kobayashi et al., 2010), and the Th2-mediated cytokine, IL-4, is involved in dicloxacillin-induced liver injury (Higuchi et al., 2011), suggesting that the pathogenesis of DILI involves an altered balance of the Th cells. However, there are a few reports of mechanistic investigations of immune-mediated DILI.

The release of a variety of inflammatory mediators would occur in DILI. The liver is selectively enriched in Kupffer cells (KCs), natural killer (NK) cells, and NK cells with T cell receptors (NKT), which are key components of the innate immune system and develop intracellular networks mediated by cytokine and chemokine signaling (Racanelli and Rehermann, 2006). Among them, KCs have been shown to participate in several types of well-known liver injury, including bile duct ligation (Souto et al., 2001) and acute alcoholic liver damage (Enomoto et al., 2000). However, the protoxicant versus protective role of KCs during acetaminophen (APAP)-induced hepatotoxicity has been widely debated (Laskin et al., 1995). In addition, previous report demonstrated that KC depletion did not affect the severity of liver injury caused by halothane (Cheng et al., 2010). Therefore, the contribution of KC in DILI is still controversial.

In this study, we first induced diclofenac-induced acute liver injury in wild-type normal mice, and demonstrated that Th17-related immunological factors are mainly involved. Furthermore, the early onset of diclofenac-induced hepatic injury was investigated.

2. Methods

2.1. Chemicals

Diclofenac sodium salt, gadolinium (III) chloride hexahydrate ($GdCl_3$) and concanavalin A (Con A) were purchased from Sigma–Aldrich (St. Louis, MO). Ibuprofen was purchased from Wako Pure Chemicals (Osaka, Japan). Fuji DRI-CHEM slides of GPT/ALT-PIII and GOT/AST-PIII to measure alanine aminotransferase (ALT) and aspartate aminotransferase (AST), respectively, were from Fujifilm (Tokyo, Japan). RNAiso was from Nippon Gene (Tokyo, Japan). ReverTra Ace was from Toyobo (Tokyo, Japan). Random hexamer and SYBR Premix Ex Taq were from Takara (Osaka, Japan). All primers were commercially synthesized at Hokkaido System Sciences (Sapporo, Japan). Rabbit polyclonal antibody against myeloperoxidase (MPO) was purchased from DAKO (Carpinteria, CA). Monoclonal anti-mouse IL-17 antibody, monoclonal anti-mouse IL-1β antibody, rat IgG2a isotype (control for the IL-17 experiment) and rat IgG1 isotype (control for the IL-1β experiment) were from R&D systems (Abingdon, UK). A Ready-SET-GO! Mouse Interleukin-17A (IL-17A) enzyme-linked immunosorbent assay (ELISA) kit and a Ready-SET-GO! Mouse Interleukin-1β (IL-1β) ELISA kit were from eBioscience (San Diego, CA). Other chemicals were of analytical or the highest grade commercially available.

2.2. Diclofenac administration

Female BALB/cCrSlc mice (8 weeks old) were obtained from SLC Japan (Hamamatsu, Japan). Mice were housed in a controlled environment (temperature 25 ± 1 °C, humidity 50 ± 10%, and 12 h light/12 h dark cycle) in the institutional animal facility with access to food and water *ad libitum*. Animals were acclimatized before use for the experiments. Diclofenac (dissolved in corn oil, *i.p.*) was administered to mice in a non-fasting condition. At the indicated time after diclofenac administration, the animals were sacrificed, and the blood was collected from the inferior vena cava and the liver from the biggest lobe. A portion of each excised liver was fixed in 10% formalin neutral buffer solution and used for immunohistochemical staining. The degree of liver injury was assessed by hematoxylin–eosin (H&E) staining. Infiltration of mononuclear cells was assessed by immunostaining for myeloperoxidase (MPO). Rabbit polyclonal antibody against MPO was used for immunohistochemical staining of the liver as previously described (Kumada et al., 2004). Animal maintenance and treatment were conducted in accordance with the National Institutes of Health Guide for Animal Welfare of Japan, as approved by the Institutional Animal Care and Use Committee of Kanazawa University, Japan (AP-111985).

Table 1
Sequences of primers used for real-time RT-PCR analyses.

Target		Sequence
mFasL	FP	5′-AGA AGG AAC TGG CAG AAC TC-3′
	RP	5′-GCG GTT CCA TAT GTG TCT TC-3′
mGATA-3	FP	5′-GGA GGA CTT CCC CAA GAG CA-3′
	RP	5′-CAT GCT GGA AGG GTG GTG A-3′
mIFN-γ	FP	5′-GGC CAT CAG CAA CAT AAG C-3′
	RP	5′-TGG ACC ACT CGG ATG AGC TCA-3′
mIL-1β	FP	5′-GTT GAC GGA CCC CAA AAG AT-3′
	RP	5′-CAC ACA CCA GCA GGT TAT CA-3′
mMCP-1	FP	5′-TGT CAT GCT TCT GGG CCT G-3′
	RP	5′-CCT CTC TCT TGA GCT TGG TG-3′
mMIP-2	FP	5′-AAG TTT GCC TTG ACC CTG AAG-3′
	RP	5′-ATC AGG TAC GAT CCA GGC TTC-3′
mROR-γt	FP	5′-ACC TCC ACT GCC AGC TGT GTG CTG TC-3′
	RP	5′-TCA TTT CTG CAC TTC TGC ATG TAG ACT GTC CC-3′
mSTAT1	FP	5′-GTT TCA GCT CTG CTC CAT AC-3′
	RP	5′-CTG CTG AAG CTC GAA CCA C-3′
mSTAT3	FP	5′-TGC AGA GCA GGT ATC TTG AG-3′
	RP	5′-TGC TGC TTC TCT GTC ACT AC-3′
mSTAT6	FP	5′-ATC TTC AAC GAC AAC AGC CTC A-3′
	RP	5′-GGA GAA GGC TAG TGA CAT ATT G-3′
mT-bet	FP	5′-CAA GTG GGT GCA GTG TGG AAA G-3′
	RP	5′-TGG AGA GAC TGC AGG ACG ATC-3′
mTNFα	FP	5′-TGT CTC AGC CTC TTC TCA TTC C-3′
	RP	5′-TGA GGG TCT GGG CCA TAG AAC-3′
mGapdh	FP	5′-AAA TGG GGT GAG GCC GGT-3′
	RP	5′-ATT GCT GAC AAT CTT GAG TGA-3′

FP, forward primer; RP, reverse primer.

2.3. Real-time reverse transcription (RT)-PCR

RNA from the mouse liver was isolated using RNAiso according to the manufacturer's instructions. The expressions of T-bet, ROR-γt, GATA-3, IFN-γ, IL-1β, Fas ligand (FasL), STAT1, STAT3, STAT6, tumor necrosis factor (TNF) α, monocyte chemoattractant protein-1 (MCP-1), and macrophage inflammatory protein (MIP)-2 were quantified by real-time RT-PCR. The primer sequences used in this study are shown in Table 1. For the RT-process, total RNA (10 μg) and 150 ng random hexamer were mixed and incubated at 70 °C for 10 min. RNA solution was added to a reaction mixture containing 100 units of ReverTra Ace, reaction buffer and 0.5 mM dNTPs in a final volume of 40 μl. The reaction mixture was incubated at 30 °C for 10 min, 42 °C for 1 h, and heated at 98 °C for 10 min to inactivate the enzyme. The real-time RT-PCR was performed using the Mx3000 P instrument (Stratagene, La Jolla, CA). The PCR mixture contained 1 μl of template cDNA, SYBR Premix Ex Taq solution and 8 pmol of forward and reverse primers. Amplified products were monitored directly by measuring the increase of the dye intensity of the SYBR Green I (Molecular Probes, Eugene, OR).

2.4. Administration of anti-mouse IL-17 antibody or anti-mouse IL-1β antibody

Anti-mouse IL-17 antibody or rat IgG2a isotype control (0.1 mg per mouse in PBS, i.v.) was administered to mice 6 h after the diclofenac administration (80 mg/kg, *i.p.*) in a non-fasting condition. Anti-mouse IL-1β antibody or rat IgG1 isotype control (0.1 mg per mouse in PBS, *i.p.*) was administered to mice 1 h prior to the diclofenac administration (80 mg/kg, *i.p.*) to mice in a nonfasting condition. Twenty-four hours after the diclofenac administration, the plasma ALT level was measured.

2.5. Measurement of plasma IL-17 and IL-1β levels

The plasma IL-17 and IL-1β levels were measured by ELISA using a kit according to the manufacturer's instructions.

2.6. Kupffer cells depletion

To deplete hepatic KCs, $GdCl_3$ (20 mg/kg, *i.v.*) was administered to mice 24 h prior to diclofenac (80 mg/kg, *i.p.*) or Con A administration (25 mg/kg in saline, *i.v.*). Twenty-four hours after diclofenac administration, the plasma ALT level was measured. As a positive control, Con A was administered to mice, and the plasma ALT level was measured 12 h after the Con A administration.

2.7. Statistical analysis

Data are presented as mean ± SD. Statistical analyses between multiple groups were performed using one-way analysis of variance (ANOVA), followed by Tukey's post hoc test. Comparisons between two groups were carried out using two-tailed Student *t*-test. $p < 0.05$ was considered statistically significant.

3. Results

3.1. Dose- and time-dependent hepatotoxic effects of diclofenac in mice

Diclofenac was administered intraperitoneally at a dose of 50, 80, or 120 mg/kg to female BALB/c mice. Ibuprofen (120 mg/kg) was used as a negative control. Plasma ALT and AST levels were significantly increased in mice administered doses of 80 and 120 mg/kg compared with vehicle-administered control mice (Fig. 1A). No hepatotoxic effect was observed in ibuprofen-administered mice. A dose-dependent increase of ALT and AST was demonstrated at a dose of 80 mg/kg, thus we adapted a dose of 80 mg/kg in the subsequent experiments. The time-dependent hepatotoxic effect of diclofenac was investigated at a dose of 80 mg/kg (Fig. 1B). A slight increase of plasma ALT and AST levels 1 h after the administration, and a marked increase of the ALT and AST levels 24 h after the administration were observed, which then decreased after 24 h. Histopathological examination of liver tissues 24 h after diclofenac administration (80 mg/kg) indicated necrosis and apoptosis (Fig. 1C). In the anti-MPO antibody staining, infiltration of mononuclear cells into the hepatocytes was observed in the diclofenac-administered mice, but not in the vehicle-administered mice.

3.2. Time-dependent changes of the mRNA expression of immune-related transcriptional factors and immune-related factors in diclofenac-administered mouse liver

To investigate the involvement of immune-related factors in the diclofenac-induced hepatotoxicity, the hepatic mRNA expression of immune-related transcriptional factors of Th cells (T-bet, GATA-3, ROR-γt, STAT1, STAT3, STAT6) and inflammatory mediators (IL-1β, TNFα, IFN-γ, MIP-2, MCP-1, FasL) was measured by real-time RT-PCR (Figs. 2 and 3). In our previous studies (Higuchi et al., 2011; Kobayashi et al., 2010), we confirmed that the expression levels of mRNA and protein were similar in ILs and chemokines. Thus, changes of mRNA expression were mainly followed in the present study, except those of some ILs. The hepatic mRNA expressions of Th17 cell-related factors, such as ROR-γt and STAT3, were significantly increased in diclofenac-administered mice compared with the control mice, whereas the expressions of Th1 cell-related factors of STAT1 and T-bet were significantly decreased, while Th2 cell-related factors (GATA3 and STAT6) were not changed (Fig. 2). As shown in Fig. 3, expressions of IL-1β, TNFα, MIP-2, MCP-1, and FasL mRNA expressions were significantly increased in diclofenac-administered mice compared with the control mice, whereas IFN-γ expression was significantly decreased 24 h after diclofenac administration. In particular, IL-1β expression was significantly increased from 3 to 12 h after the administration and peaked at 3 h, suggesting that IL-1β might be related to the early onset of diclofenac-induced liver injury.

3.3. Involvement of IL-17 in diclofenac-induced liver injury

IL-17 is a cytokine, mainly produced by Th17 cells (Nakae et al., 2003), which can induce inflammatory cytokines and chemokines (Yao et al., 1995). Plasma IL-17, measured by ELISA, was detected in mice 24 and 36 h after the diclofenac administration (Fig. 4A), but not in the control mice. The IL-17 neutralization study demonstrated that the administration of anti-mouse IL-17 antibody (0.1 mg/mouse, *i.v.*) 6 h after diclofenac administration resulted in lower levels of the plasma ALT compared with that of IgG2a-treated control mice (Fig. 4B). Plasma IL-17 level in anti-mouse IL-17 antibody-treated mice was significantly decreased compared with mice administered diclofenac alone (Fig. 4C).

3.4. Role of KCs in diclofenac-induced liver injury

KCs are known as one of the sources of cytokines and chemokines in the liver, which suggests that KCs would be involved in the pathogenesis of diclofenac-induced hepatotoxicity. KCs were depleted by $GdCl_3$ (20 mg/kg, *i.v.*) treatment 24 h prior to Con A or diclofenac administration. The dosing condition in this study enabled us to deplete approximately 75% of hepatic KCs (Xu et al., 2010), which attenuated Con A-induced hepatitis (Hatano et al., 2008). In this study, attenuation of the Con A-induced hepatic injury using $GdCl_3$ was demonstrated, but there was no effect on the diclofenac-induced hepatic injury (Fig. 5), suggesting that KCs are not likely involved in the pathogenesis of diclofenac-induced liver injury.

3.5. Involvement of IL-1β in the pathogenesis of diclofenac-induced liver injury

IL-1β is known as an inflammatory cytokine. In the present study, among the many ILs and chemokines, IL-1β mRNA increased early after diclofenac administration, suggesting the involvement of IL-1β in the early onset of hepatic injury. Plasma IL-1β was detected by ELISA from 6 to 36 h after the administration, and a marked increase was observed 24 h after the administration (Fig. 6A). To further investigate whether IL-1β was involved in the diclofenac-induced liver injury, we performed IL-1β neutralization studies. The administration of anti-mouse IL-1β antibody (100 μg/mouse, *i.p.*) 1 h before diclofenac administration significantly reduced the plasma ALT level at 24 h after diclofenac administration compared with IgG1-treated control mice (Fig. 6B). Plasma IL-1β level in anti-mouse IL-1β antibody-treated mice was significantly decreased compared with mice administered diclofenac alone (Fig. 6C).

4. Discussion

Diclofenac is known to cause rare but sometime serious hepatotoxicity in humans (Bhogaraju et al., 1999), but the mechanism of diclofenac-induced liver injury remained to be clarified. There is some evidence suggesting an immune-mediated reaction in diclofenac-induced hepatic injury in human (Greaves et al., 2001; Kretz-Rommel and Boelsterli, 1995). However, there was no animal model that reproduced the diclofenac-induced liver injury. These lines of background prompted us to investigate the immune-mediated mechanisms in diclofenac-induced liver injury.

First, we established the dosing condition for diclofenac-induced acute liver injury in mice. In general, the route of drug administration in clinical practice is an ideal pathway to develop an animal model. However, diclofenac is known to cause gastrointestinal toxicity (Novartis Pharma Co, 2005). Therefore, we adapted *i.p.* administration of diclofenac to avoid gastrointestinal toxicity, as possible. Previous studies demonstrated that diclofenac administration (100 mg/kg dissolved in saline, *i.p.*) caused only a slight increase in the serum ALT level in rat (Deng et al., 2006). Acute toxicity study demonstrated that the LD_{50} value of single *i.p.* administration of diclofenac in female mice was 250 mg/kg (Novartis Pharma Co, 2005). Therefore, in the present study, single *i.p.* administration of diclofenac at dose of 50, 80, and 120 mg/kg,

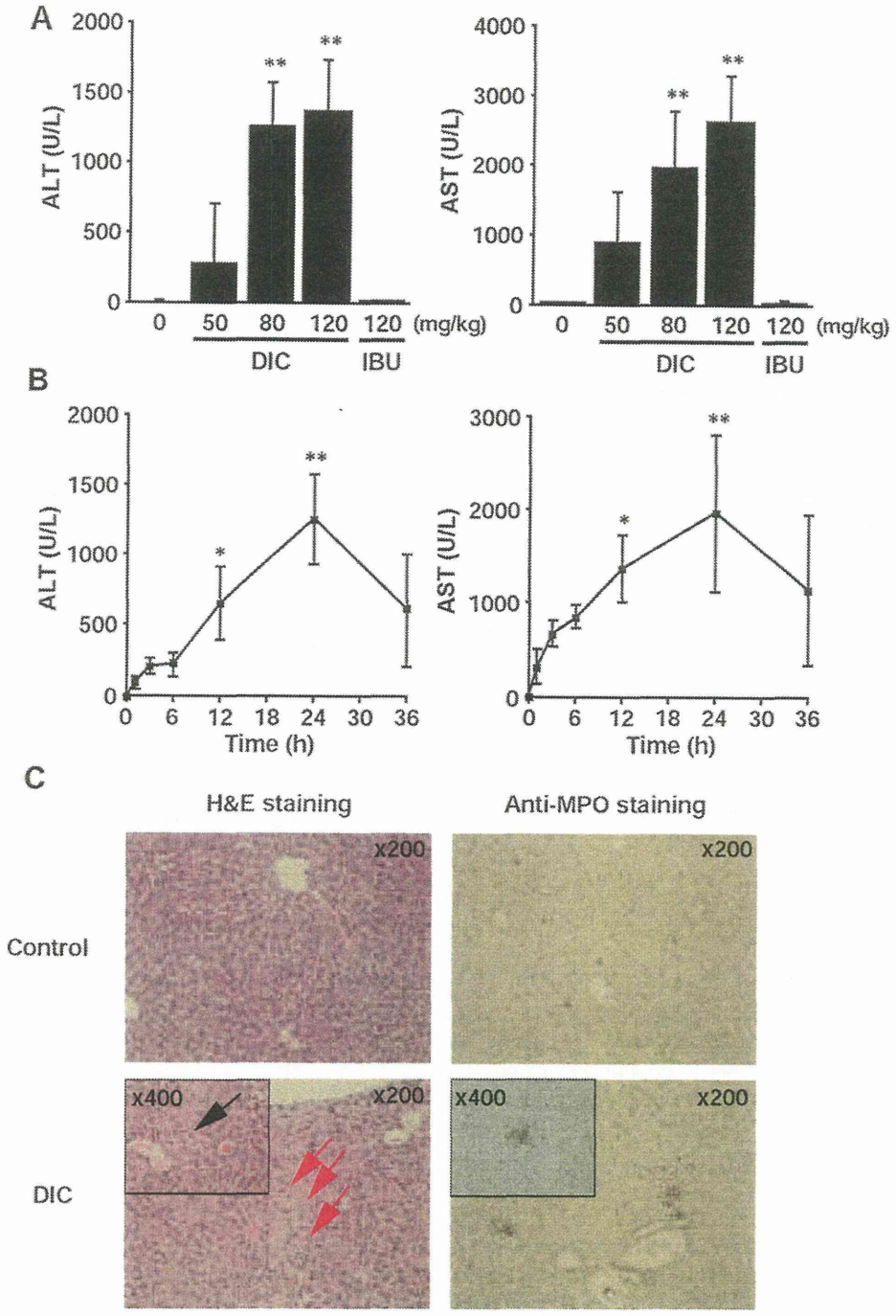

Fig. 1. Dose- and time-dependent changes of plasma ALT and AST and histopathological examination in the liver of diclofenac-administered mice. (A) Diclofenac (DIC: 50, 80, or 120 mg/kg in corn oil, *i.p.*) or ibuprofen (IBU: 120 mg/kg in corn oil, *i.p.*) was administered to mice, and plasma samples were collected for the assessment of ALT and AST 24 h after the administration. (B) Diclofenac (80 mg/kg, *i.p.*) was administered to mice and plasma samples were collected 1, 3, 6, 12, 24 and 36 h after the administration. Data are mean ± SD ($n = 4–5$). Significantly different from vehicle-administered control mice (*$p < 0.05$, **$p < 0.01$). (C) Histopathological examination of the livers from diclofenac-administered mice. Liver specimens were examined 24 h after the diclofenac administration (80 mg/kg). The liver sections were stained with H&E or immunostained with anti-MPO antibody. Black arrow indicates apoptotic cells and red arrows indicate necrotic cells.

which is less than a half of the *i.p.* LD_{50}, was adapted. After investigating many different conditions, we found that administration of diclofenac 80 mg/kg dissolved in corn oil (*i.p.*) without fasting condition, reproducibly caused diclofenac-induced acute liver injury in mice. Ibuprofen, having similar pharmacological properties as diclofenac, is known to be less hepatotoxic than diclofenac (Rainsford, 2009). Ibuprofen showed no hepatotoxic effect in the same dosing condition as diclofenac, suggesting that the pharmacological effects may not contribute to the diclofenac hepatotoxicity in this model.

In this study, a relationship between diclofenac-induced liver injury and immune-related factors was demonstrated. The administration of diclofenac significantly increased the expression of hepatic ROR-γt and STAT3 mRNA, as well as the plasma IL-17 level (Figs. 2 and 4A). ROR-γt is a master regulator in Th17 cells (Kidd, 2003; Steinman, 2007). STAT3 is also required for the development

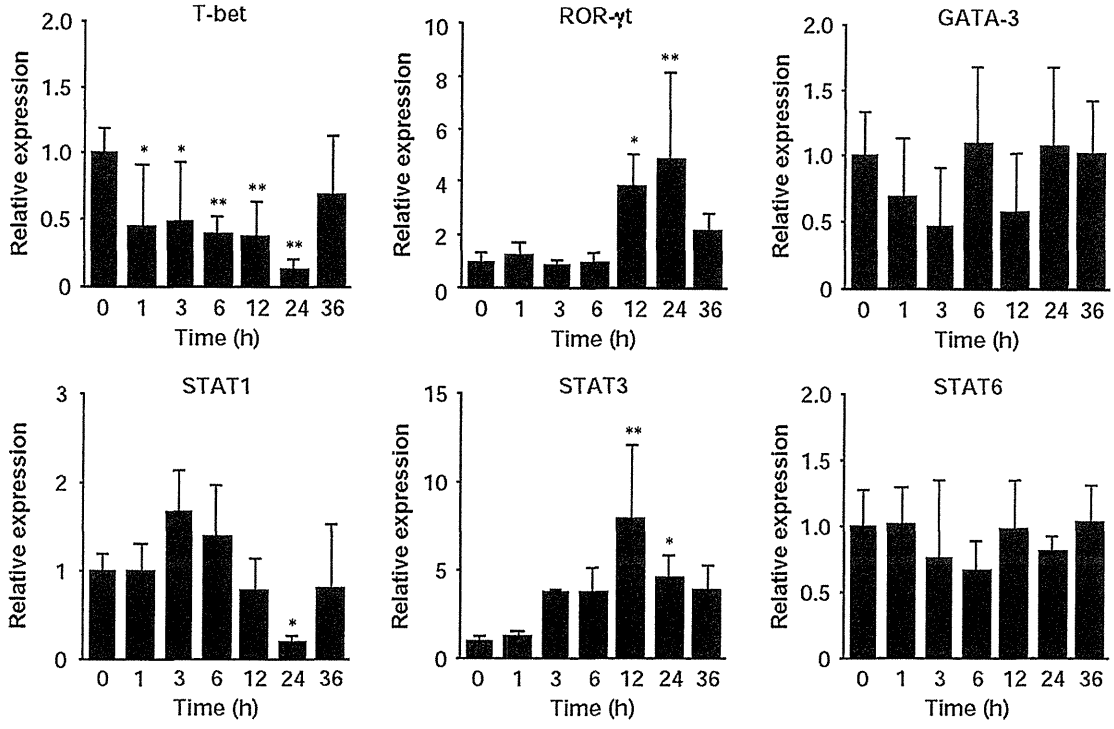

Fig. 2. Time-dependent changes in hepatic mRNA expression of CD4⁺ Th cells-related transcriptional factors in diclofenac-administered mice. Diclofenac (80 mg/kg, *i.p.*) was administered to mice. After 1, 3, 6, 12, 24, and 36 h, the expressions of T-bet, ROR-γt, GATA-3, STAT1, STAT3, and STAT6 mRNA in the liver were measured by real-time RT-PCR. The expression of hepatic mRNA was normalized to the expression of Gapdh mRNA. Data are mean ± SD (n = 4–5). Significantly different from control (0 h) mice ($^{*}p < 0.05$, $^{**}p < 0.01$).

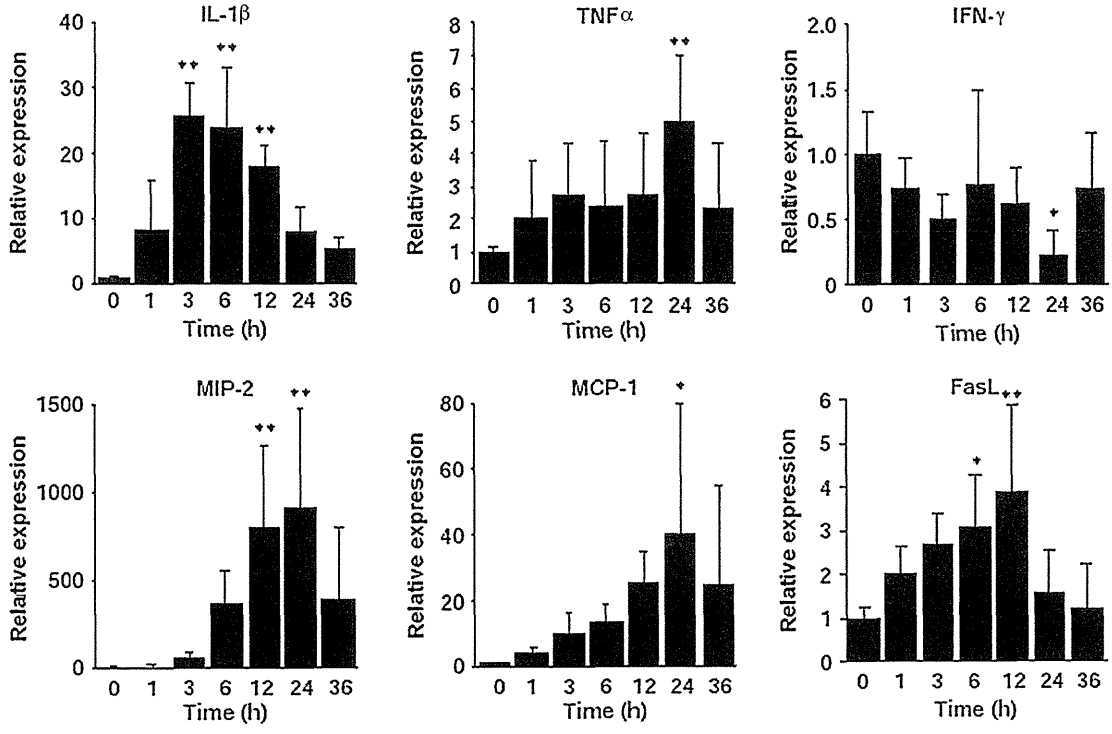

Fig. 3. Time-dependent changes in hepatic mRNA expression levels of cytokines and chemokines in diclofenac-administered mice. Diclofenac (80 mg/kg, *i.p.*) were administered to mice. After 1, 3, 6, 12, 24, and 36 h, the hepatic expressions of IL-1β, TNFα, INF-γ, MIP-2, MCP-1, and FasL mRNA in the liver were measured by real-time RT-PCR. The expression of hepatic mRNA was normalized to the expression of Gapdh mRNA. Data are mean ± SD (n = 4–5). Significantly different from control (0 h) mice ($^{*}p < 0.05$, $^{**}p < 0.01$).

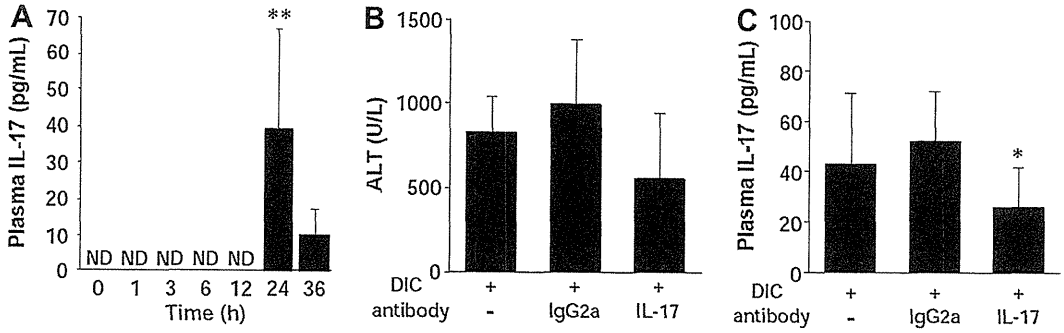

Fig. 4. Time-dependent changes of the plasma IL-17 level and effect of anti-IL-17 antibody administration to diclofenac-administered mice. (A) The plasma IL-17 level was measured by ELISA 1, 3, 6, 12, 24, and 36 h after diclofenac administration (80 mg/kg, *i.p.*). Data are mean ± SD (n = 4–5). (B) Six hours after diclofenac (DIC) administration (80 mg/kg, *i.p.*), IgG2a (control) or anti-mouse IL-17 antibody (0.1 mg/mouse, *i.v.*) was administered. The plasma ALT level was measured 24 h after diclofenac administration. Data are mean ± SD (n = 8–10). (C) The plasma IL-17 level after administered of anti-mouse IL-17 specific antibody or IgG2a was measured by ELISA 24 h after diclofenac administration (80 mg/kg, *i.p.*). Data are mean ± SD (n = 8–10). Significantly different from control (0 h) mice (*p < 0.05, **p < 0.01).

of Th17 cells, and STAT3 deficiency impairs ROR-γt expression (Harris et al., 2007; Yang et al., 2007). It has been suggested that Th17 cell-mediated factors are partly involved in diclofenac-induced hepatotoxicity. It has been reported that the plasma IL-17 levels were elevated in 60% of patients with DILI and occasionally in patients with viral hepatitis (Li et al., 2009), suggesting IL-17 might have a role in liver injury in human.

In our previous study using a halothane-induced liver injury mouse model (Kobayashi et al., 2009), we found that the appropriate dose of anti-IL-17 antibody to suppress the hepatotoxic effect is 100 μg/body. Neutralization of IL-17 tended to inhibit the increase of the plasma ALT level (Fig. 4B), suggesting that IL-17 was partly involved in the diclofenac-induced hepatic injury.

Cytokines and chemokines such as TNFα, IL-1β, MIP-2, and MCP-1 were significantly increased in the diclofenac-administered mice (Fig. 3). TNFα is a pleiotropic pro-inflammatory cytokines produced by a variety of cell types including macrophages, T cells, and mast cells (Tracey, 1994). MCP-1 is increased in APAP-induced liver injury (Dambach et al., 2006), and MIP-2 induces neutrophil recruitment and is markedly increased in halothane-induced hepatotoxicity (Kobayashi et al., 2009). From these lines of data into consideration, it is known that two death receptor ligands, TNFα or FasL, bind to their receptors and induce apoptosis (Nagata, 1997). The expression of hepatic TNFα and FasL mRNA was significantly increased, and hepatocellular apoptosis were observed (Figs. 1C and 3), suggesting that these mediators may cause hepatocellular apoptosis in diclofenac-induced liver injury. Thus, the exacervation of diclofenac-induced liver injury could involve these mediators.

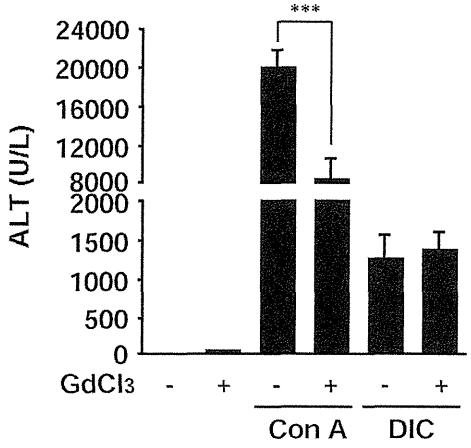

Fig. 5. Role of KCs in diclofenac-induced liver injury. $GdCl_3$ (20 mg/kg, *i.v.*) were administered to mice 24 h prior to diclofenac (80 mg/kg, *i.p.*) or Con A (25 mg/kg, *i.v.*) administration. The Plasma ALT level was measured 24 h after diclofenac administration or 12 h after Con A administration. Data are mean ± SD (n = 4–5). Significantly different from control (without $GdCl_3$ administration) mice (***p < 0.001).

KCs serve important regulatory functions in pathophysiological states of the liver and have the ability to produce a range of inflammatory mediators, including TNFα and IL-1β. It is also reported that KCs play a dispensable role in the development of halothane hepatotoxicity (Cheng et al., 2010). The dosing condition of $GdCl_3$ in this study was determined according to Xu et al.

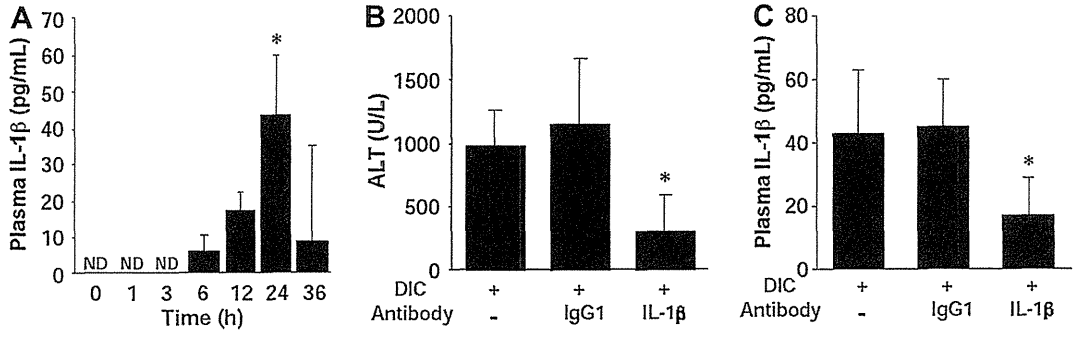

Fig. 6. Time-dependent change of plasma IL-1β level and effect of anti-IL-1β antibody administration to diclofenac-administered mice. (A) The plasma IL-1β level was measured by ELISA 1, 3, 6, 12, 24, and 36 h after diclofenac (80 mg/kg, *i.p.*) administration. (B) One hour before the diclofenac (80 mg/kg, *i.p.*) administration, IgG1 (control) or anti-mouse IL-1β antibody (0.1 mg/mouse, *i.p.*) was administered. The plasma ALT level was measured 24 h after the diclofenac administration. (C) The plasma IL-1β level after administered anti-mouse IL-1β specific antibody or IgG1 was measured by ELISA 24 h after diclofenac administration (80 mg/kg, *i.p.*). Data are mean ± SD (n = 4–5). Significantly different from control mice (A) or IgG1-administered mice (B and C) (*p < 0.05). ND: not detected.

(2010). To confirm whether $GdCl_3$ administration resulted in the depletion of KCs, we revealed the attenuation of Con A-induced hepatitis by $GdCl_3$ (Fig. 5), and the attenuation of plasma ALT was also observed 24 h after Con A administration (data not shown). In this study, we demonstrated that KCs are not likely to be involved in the pathogenesis of diclofenac hepatotoxicity.

In the present study, the increase of hepatic IL-1β mRNA expression and plasma IL-1β level was observed soon after the diclofenac administration (Figs. 3 and 6A). IL-1β is a very potent pro-inflammatory cytokine and the primary sources of IL-1β are blood monocytes and dendritic cells. Hepatocytes and neutrophils also produce IL-1β (Arend et al., 2008). IL-1β acts mainly as a pro-inflammatory mediator activating and recruiting leukocytes, especially neutrophils, into the liver (Bajt et al., 2001). It is well known that activated neutrophils release protease such as elastase that can cause tissue injury. Within the liver, activated neutrophils act as effector cells through cytotoxicity, leading hepatocyte necrosis. In a number of experimental animal models, accumulated neutrophils in the liver were reported to contribute to the progression and severity of a number of experimental animal models such as ischemia-reperfusion injury (Jaeschke et al., 1990; Ramaiah and Jaeschke, 2007), and APAP- and halothane-induced hepatotoxicity (Liu et al., 2006; You et al., 2006). In the present study, neutrophil infiltration occurred in the diclofenac-administered mouse liver (Fig. 1C), and neutralization of IL-1β attenuated diclofenac-induced hepatotoxicity (Fig. 6), suggesting that IL-1β is involved in the early onset of diclofenac-induced liver injury.

A previous study demonstrated a significant increase of reactive oxygen species (ROS) in hepatocytes treated with diclofenac (Gómez-Lechón et al., 2003). Increased ROS levels can trigger "NACHT, LRR, and pyrin domain-containing protein 3" (NALP3) inflammasome activation, which is a multimetimeric protein complex that mediates the processing of the pro-inflammatory caspases and cytokines, such as IL-1β (Agostini et al., 2004). The IL-1β levels are known to be increased during APAP hepatotoxicity (Cover et al., 2006) and halothane-induced liver injury (Toyoda et al., 2011). Therefore, it is conceivable that IL-1β would be released into the extracellular environment by oxidative stress such as ROS and activates immune cells.

In conclusion, we developed a diclofenac-induced acute liver injury model in mice, and demonstrated that Th17-related immunological factors are significantly increased. Furthermore, IL-1β appeared to be involved in the early onset of diclofenac-induced hepatic injury. These findings may shed light on the mechanisms of DILI.

Funding Information

Health and Labor Sciences Research Grants from the Ministry of Health, Labor and Welfare of Japan (H23-BIO-G001).

Conflict of interest statement

The authors declare that there are no conflicts of interest.

Acknowledgment

We thank Mr. Brent Bell for reviewing the manuscript.

References

Agostini, L., Martinon, F., Burns, K., McDermott, M.F., Hawkins, P.N., Tschopp, J., 2004. NALP3 forms an IL-1β-processing inflammasome with increased activity in Muckle-Wells autoinflammatory disorder. Immunity 20, 319–325.
Arend, W.P., Palmer, G., Gabay, C., 2008. IL-1, IL-18, and IL-33 families of cytokines. Immunol. Rev. 223, 20–38.
Bajt, M.L., Farhood, A., Jaeschke, H., 2001. Effects of CXC chemokines on neutrophil activation and sequestration in hepatic vasculature. Am. J. Physiol. Gastrointest. Liver Physiol. 281, G1188–G1195.
Bhogaraju, A., Nazeer, S., A.L-Baghdadi, Y., Rahman, M., Wrestler, F., Patel, N., 1999. Diclofenac-associated hepatitis. South. Med. J. 92, 711–713.
Boelsterli, U.A., 2003. Diclofenac-induced liver injury: a paradigm of idiosyncratic drug toxicity. Toxicol. Appl. Pharmacol. 192, 307–322.
Cheng, L., You, Q., Yin, H., Holt, M.P., Ju, C., 2010. Involvement of natural killer T cells in halothane-induced liver injury in mice. Biochem. Pharmacol. 80, 255–261.
Cover, C., Liu, J., Farhood, A., Malle, E., Waalkes, M.P., Bajt, M.L., Jaeschke, H., 2006. Pathophysiological role of the acute inflammatory response during acetaminophen hepatotoxicity. Toxicol. Appl. Pharmacol. 216, 98–107.
Dambach, D.M., Durham, S.K., Laskin, J.D., Laskin, D.L., 2006. Distinct roles of NF-κB p50 in the regulation of acetaminophen-induced inflammatory mediator production and hepatotoxicity. Toxicol. Appl. Pharmacol. 211, 157–165.
Deng, X., Stachlewitz, R.F., Liguori, M.J., Blomme, E.A., Waring, J.F., Luyendyk, J.P., Maddox, J.F., Ganey, P.E., Roth, R.A., 2006. Modest inflammation enhances diclofenac hepatotoxicity in rats: role of neutrophils and bacterial translocation. J. Pharmacol. Exp. Ther. 319, 1191–1199.
Enomoto, N., Ikejima, K., Yamashina, S., Enomoto, A., Nishiura, T., Nishimura, T., Brenner, D.A., Schemmer, P., Bradford, B.U., Rivera, C.A., Zhong, Z., Thurman, R.G., 2000. Kupffer cell-derived prostaglandin E2 is involved in alcohol-induced fat accumulation in rat liver. Am. J. Physiol. Gastrointest. Liver Physiol. 279, G100–G106.
Gómez-Lechón, M.J., Ponsoda, X., O'Connor, E., Donato, T., Castell, J.V., Jover, R., 2003. Diclofenac induces apoptosis in hepatocytes by alteration of mitochondrial function and generation of ROS. Biochem. Pharmacol. 66, 2155–2167.
Greaves, R.R., Agarwal, A., Patch, D., Davies, S.E., Sherman, D., Reynolds, N., Rolles, K., Davidson, B.R., Burroughs, A.K., 2001. Inadvertent diclofenac rechallenge from generic and non-generic prescribing, leading to liver transplantation for fulminant liver failure. Eur. J. Gastroenterol. Hepatol. 13, 71–73.
Harris, T.J., Grosso, J.F., Yen, H.R., Xin, H., Kortylewski, M., Albesiano, E., Hipkiss, E.L., Getnet, D., Goldberg, M.V., Maris, C.H., Housseau, F., Yu, H., Pardoll, D.M., Drake, C.G., 2007. Cutting edge: an *in vivo* requirement for STAT3 signaling in TH17 development and TH17-dependent autoimmunity. J. Immunol. 179, 4313–4317.
Hatano, M., Sasaki, S., Ohata, S., Shiratsuchi, Y., Yamazaki, T., Nagata, K., Kobayashi, Y., 2008. Effects of Kupffer cell-depletion on concanavalin A-induced hepatitis. Cell. Immunol. 251, 25–30.
Higuchi, S., Kobayashi, M., Yoshikawa, Y., Tsuneyama, K., Fukami, T., Nakajima, M., Yokoi, T., 2011. IL-4 mediates dicloxacillin-induced liver injury in mice. Toxicol. Lett. 200, 139–145.
Holt, M.P., Ju, C., 2006. Mechanisms of drug-induced liver injury. AAPS J. 8, E48–E54.
Jaeschke, H., Farhood, A., Smith, C.W., 1990. Neutrophils contribute to ischemia/reperfusion injury rat liver *in vivo*. FASEB J. 4, 3355–3359.
Kidd, P., 2003. Th1/Th2 balance: the hypothesis, its limitations, and implications for health and disease. Altern. Med. Rev. 8, 223–246.
Kita, H., Macky, I.R., Van De Water, J., Gershwin, M.E., 2001. The lymphoid liver: considerations on pathways to autoimmune injury. Gastroenterology 120, 1485–1501.
Kobayashi, E., Kobayashi, M., Tsuneyama, K., Fukami, T., Nakajima, M., Yokoi, T., 2009. Halothane-induced liver injury is mediated by interleukin-17 in mice. Toxicol. Sci. 111, 302–310.
Kobayashi, M., Higuchi, S., Mizuno, K., Tsuneyama, K., Fukami, T., Nakajima, M., Yokoi, T., 2010. Interleukin-17 is involved in α-naphthylisothiocyanate-induced liver injury in mice. Toxicology 275, 50–57.
Kretz-Rommel, A., Boelsterli, U.A., 1995. Cytotoxic activity of T cells and non-T cells from diclofenac-immunized mice against cultured syngeneic hepatocytes exposed to diclofenac. Hepatology 22, 213–222.
Kumada, T., Tsuneyama, K., Hatta, H., Ishizawa, S., Takano, Y., 2004. Improved 1-h rapid immunostaining method using intermittent microwave irradiation: practicability based on 5 years application in Toyama Medical and Pharmaceutical University Hospital. Mod. Pathol. 17, 1141–1149.
Laskin, D.L., Gardner, C.R., Price, V.F., Jollow, D.J., 1995. Modulation of macrophage functioning abrogates the acute hepatotoxicity of acetaminophen. Hepatology 21, 1045–1050.
Leonard, W.J., O'Shea, J.J., 1998. Jaks and STATs: biological implications. Annu. Rev. Immunol. 16, 293–322.
Li, J., Zhu, X., Liu, F., Cai, P., Sanders, C., Lee, W.M., Uetrecht, J., 2009. Cytokine and autoantibody patterns in acute liver failure. J. Immunotoxicol. 7, 157–164.
Liu, Z.X., Han, D., Gunawan, B., Kaplowitz, N., 2006. Neutrophil depletion protects against murine acetaminophen hepatotoxicity. Hepatology 43, 1220–1230.
McGeachy, M.J., Cua, D.J., 2008. Th17 cell differentiation: the long and winding road. Immunity 28, 445–453.
Nagata, S., 1997. Apoptosis by death factor. Cell 88, 355–365.
Nakae, S., Nambu, A., Sudo, K., Iwakura, Y., 2003. Suppression of immune induction of collagen-induced arthritis in IL-17-deficient mice. J. Immunol. 171, 6173–6177.
Novartis Pharma Co., 2005. Interview Form (Product Information Booklet) of Voltaren®, ninth ed., Tokyo, Japan.
Purcell, P., Henry, D., Melville, G., 1991. Diclofenac hepatitis. Gut 32, 1381–1385.
Racanelli, V., Rehermann, B., 2006. The liver as an immunological organ. Hepatology 43, 54–62.
Rainsford, K.D., 2009. Ibuprofen: pharmacology, efficacy and safety. Inflammopharmacology 17, 275–342.
Ramaiah, S.K., Jaeschke, H., 2007. Role of neutrophils in the pathogenesis of acute inflammatory liver injury. Toxicol. Pathol. 35, 757–766.

Souto, E.O., Miyoshi, H., Dubois, R.N., Gores, G.J., 2001. Kupffer cell-derived cyclooxygenase-2 regulates hepatocyte Bcl-2 expression in choledocho-venous fistula rats. Am. J. Physiol. Gastrointest. Liver. Physiol. 280, G805–G811.
Steinman, L., 2007. A brief history of Th17, the first major revision in the Th1/Th2 hypothesis if T cell-mediated tissue damage. Nat. Rev. Med. 13, 139–145.
Tang, W., Stearns, R.A., Wang, R.W., Chiu, S.H., Baillie, T.A., 1999. Roles of human hepatic cytochrome P450s 2C9 and 3A4 in the metabolic activation of diclofenac. Chem. Res. Toxicol. 12, 192–199.
Toyoda, Y., Miyashita, T., Endo, S., Tsuneyama, K., Fukami, T., Nakajima, M., Yokoi, T., 2011. Estradiol and progesterone modulate halothane-induced liver injury in mice. Toxicol. Lett. 204, 17–24.
Tracey, K.J., 1994. Tumor necrosis factor-α. In: Thomson, A. (Ed.), The Cytokine Handbook. Academic Press, London, pp. 289–304.
Xu, L., Qi, J., Zhao, P., Liang, X., Ju, Y., Liu, P., Liu, B., Guo, C., Zhang, L., Ma, C., Gao, L., 2010. T cell immunoglobulin- and mucin-domain-containing molecule-4 attenuates concanavalin A-induced hepatitis by regulating macrophage. J. Leukoc. Biol. 88, 329–336.
Yang, X.O., Panopoulos, A.D., Nurieva, R., Chang, S.H., Wang, D., Watowich, S.S., Dong, C., 2007. STAT3 regulates cytokine-mediated generation of inflammatory helper T cells. J. Biol. Chem. 282, 9358–9363.
Yao, Z., Fanslow, W.C., Seldin, M.F., Rousseau, A.M., Painter, S.L., Comeau, M.R., Cohen, J.I., Spriggs, M.K., 1995. Herpesvirus Saimiri encodes a new cytokine, IL-17, which binds to a novel cytokine receptor. Immunity 3, 811–821.
You, Q., Cheng, L., Reilly, T.P., Wegmann, D., Ju, C., 2006. Role of neutrophils in a mouse model of halothane-induced liver injury. Hepatology 44, 1421–1431.

Research Article

Journal of Applied Toxicology

Received: 2 September 2011, Revised: 3 January 2012, Accepted: 3 January 2012 Published online in Wiley Online Library: 9 March 2012

(wileyonlinelibrary.com) DOI 10.1002/jat.2731

Th2 cytokine-mediated methimazole-induced acute liver injury in mice

Masanori Kobayashi,[a,b] Satonori Higuchi,[a] Mika Ide,[b] Satomi Nishikawa,[b] Tatsuki Fukami,[a] Miki Nakajima[a] and Tsuyoshi Yokoi[a]*

ABSTRACT: Drug-induced liver injury (DILI) is a major safety concern in drug development and clinical practice. The pathogenesis of DILI usually involves the participation of the parent drug or metabolites that either affect cellular function or elicit an immune response. However, the mechanisms leading to DILI are unknown in most cases. Methimazole (MTZ) is used as an antithyroid drug and is well known to have induced liver injuries such as cholestatic hepatitis in a small number of human cases. Immune-mediated reactions were also suggested to play a role in MTZ-induced acute liver injury, but the mechanism underlying this process has not been elucidated. To address this issue, we measured plasma aspartate aminotransferase (AST) and alanine aminotransferase (ALT) levels, hepatic glutathione levels, hepatic expression of $CD4^+$ Th cell-related transcriptional factors, cytokines and chemokines, plasma interleukin (IL)-4 levels and histopathological changes in the liver following MTZ (450 mg kg^{-1}, p.o.) administration in mice. The hepatic expression of mRNA for Th2 cell-related factors, such as GATA-binding protein, macrophage inflammatory protein-2 (MIP-2) and plasma IL-4 levels, as well as plasma AST and ALT levels, was significantly increased in mice treated with MTZ. These changes were markedly enhanced by pre-treatment with L-buthionine sulfoximine (3 mmol kg^{-1}, i.p.) and MTZ (15 mg kg^{-1}, p.o.). Neutralization of IL-4 using a monoclonal anti-mouse IL-4 antibody (100 μg/mouse, single i.p.) suppressed the hepatotoxic effect of MTZ. In conclusion, this report is the first to demonstrate that Th2 cytokine-mediated immune responses are involved in MTZ-induced acute liver injury in mice.

Keywords: drug-induced liver injury; cytokines; IL-4; eotaxin; helper T cells

INTRODUCTION

Drug-induced liver injury (DILI) remains an important cause of acute liver failure and is a major reason for the withdrawal of approved drugs from the market. The pathogenesis of drug-induced liver injury usually involves the participation of the parent drug or metabolites that either directly affect cell functions or elicit an immune response. Some drugs, such as tienilic acid, amodiaquine and halothane, are suggested to induce immune-related DILI (Bugelski, 2005). In most cases, the mechanisms underlying DILI are unknown because predictive *in vitro* screening methods and animal models are lacking.

Methimazole (MTZ), which is widely used to treat hyperthyroidism, is well known to induce DILI, such as acute hepatic necrosis and cholestatic hepatitis, with a low incidence (Luca *et al.*, 2009; Sadoul *et al.*, 1993; Vitug and Goldman, 1985). The metabolic activation of MTZ by either hepatic cytochrome P-450 (P450) or flavin-containing monooxygenases (FMO) has been proposed to produce reactive metabolites that may covalently bind to proteins and inactive P450 (Lee and Neal, 1978; Kedderis and Rickert, 1985). It was reported that the inadequate detoxification of reactive metabolites was responsible for the hepatotoxicity observed in glutathione (GSH) depleted mouse and rat models using L-buthionine sulfoximine (BSO) (Mizutani *et al.*, 1999; Shimizu *et al.*, 2011). However, it is not clear whether immune-mediated factors are involved in MTZ-induced acute liver injury.

Although the pathogenesis of DILI is not fully understood, it can be divided into a two-stage process based on studies of the mechanisms involved in animal models (Laverty *et al.*, 2010). In the first step, chemical stress responses, such as mitochondrial dysfunction, are induced owing to excessive drug accumulation and/or metabolic activation. The second step is the process of adaptation or failure of the response mediated by immune-related cells. In addition, as knowledge concerning the role of immune cells in hepatic pathology accumulates, it is becoming clear that immune responses possibly play an essential role in DILI (Adams *et al.*, 2010). Therefore, it is important to understand the mechanisms by which cells that play a role in the immune system are activated during DILI.

Helper T cells ($CD4^+$ Th cells) are an important regulator in the pathogenesis of a variety of human liver disorders (Kita *et al.*, 2001; Heneghan and McFarlane, 2002). The action of T cells in the liver is mediated through the release of a variety of cytokines that target liver cells and immune cells by activating multiple signaling cascades (Leonard and O'Shea, 1998). Th cells are subdivided into Th1, Th2, regulatory T cells (Treg) and Th17 based on their unique production of cytokines and characteristic transcription factors (Kidd,

* *Correspondence to: Tsuyoshi Yokoi, Drug Metabolism and Toxicology, Faculty of Pharmaceutical Sciences, Kanazawa University, Kakuma-machi, Kanazawa 920–1192, Japan.*
E-mail: tyokoi@kenroku.kanazawa-u.ac.jp

[a] *Drug Metabolism and Toxicology, Faculty of Pharmaceutical Sciences, Kanazawa University, Kanazawa, 920-1192, Japan*

[b] *Research Division, Mitsubishi Tanabe Pharma. Co., Kisarazu, Chiba 292-0818, Japan*

2003; Zhu and Paul, 2008). Th1 cells require 'T-box expressed in T cells' (T-bet) and secrete interferon (IFN)-γ. Th2 cells require GATA-binding domain-3 (GATA-3) and produce IL-4 and IL-5. In addition, Th17 cells secrete IL-17 and IL-22 require 'retinoid-related orphan receptor γt' (ROR-γt) for differentiation (Zhu and Paul, 2008).

Th2 cell-mediated responses influence a wide range of events associated with allergic inflammation via IL-4 and IL-5. IL-4 promotes the development of mast cells. IL-5 is involved in the development of eosinophils (Kay, 2001). In concanavalin (Con) A-mediated hepatitis, a widely accepted mouse model for studying T cell-mediated liver injury, IL-4 stimulates the secretion of eotaxin-1 and enhances IL-5 production, resulting in attraction of neutrophils and eosinophils to the liver, which leads to hepatitis (Jaruga *et al.*, 2003).

We recently reported that IL-17 is involved in halothane- and α-naphthylisothiocyanate-induced acute liver injury in mice (Kobayashi *et al.*, 2009, 2010) and that IL-4 is involved in dicloxacillin-induced acute liver injury in mice (Higuchi *et al.*, 2011). In this study, we found that Th2 cytokine-mediated immune responses play a role in MTZ-induced acute liver injury in mice.

MATERIALS AND METHODS

Materials

MTZ and BSO were purchased from Sigma-Aldrich (St Louis, MO, USA). GSH was obtained from Wako Pure Chemical Industries (Osaka, Japan). β-NADPH and GSH reductase came from Oriental Yeast (Tokyo, Japan). RNAiso came from Nippon Gene (Tokyo, Japan). ReverTra Ace came from Toyobo (Tokyo, Japan). Random hexamers and SYBR Premix Ex Taq were from Takara (Osaka, Japan). All primers were commercially synthesized at Hokkaido System Sciences (Sapporo, Japan). A rabbit polyclonal antibody against myeloperoxidase (MPO) was obtained from Thermo Fisher Scientific Anatomical Pathology (Cheshire, UK). A monoclonal anti-mouse IL-4 antibody came from U-Cytech Biosciences (Utrecht, Netherland). A monoclonal rat IgG2a isotype, used as a negative control, was purchased from R&D Systems (Abingdon, UK). A Ready-SET-GO! Mouse IL-4 enzyme-linked immunosorbent assay (ELISA) kit was obtained from eBioscience (San Diego, CA, USA). Fuji DRI-CHEM slides of GPT/ALT-PIII and GOT/AST-PIII, which were used to measure alanine aminotransferase (ALT) and aspartate aminotransferase (AST), respectively, came from Fujifilm (Tokyo, Japan). Other chemicals used were of analytical or the highest grade commercially available.

MTZ Administration

Female BALB/cCrSlc mice (6 weeks old, 15–20 g) were obtained from SLC Japan (Hamamatsu, Japan). The animals were housed in a controlled environment (temperature 25 ± 1 °C, humidity 50 ± 10%, 12 h light/12 h dark cycle) in the institution's animal facility with *ad libitum* access to food and water. The animals were acclimatized before use in the experiments. MTZ was dissolved in saline (45 mg ml^{-1}) and administered orally to the mice at a dose of 450 or 15 mg kg^{-1} following overnight fasting. Two hours after MTZ administration, the mice were again allowed access to food and water *ad libitum*. Animal maintenance and treatments were conducted in accordance with the National Institutes of Health Guide for Animal Welfare of Japan, as approved by the Institutional Animal Care and Use Committee of Kanazawa University, Japan.

An MTZ dose of 450 mg kg^{-1} was set at approximately one-half the oral LD_{50} value based on the results of experiments to determine the effects of MTZ doses of 860 (the oral LD_{50} in mice), 450 and 225 mg kg^{-1} as follows. It was difficult to assess the hepatotoxicity of MTZ at a dose of 860 mg kg^{-1} because symptoms of moribundity, such as decreased locomotor activity and tremor, were observed in all mice treated with MTZ at this dose. In addition, plasma AST and ALT values exhibited a high degree of individual variation (AST and ALT values were 3165 ± 7175 and 4087 ± 8063 IU l^{-1}, respectively). There was no difference in plasma AST and ALT values between the MTZ 450 mg kg^{-1} (AST and ALT values were 104 ± 29 and 79 ± 4 IU l^{-1}, respectively) and MTZ 225 mg kg^{-1} groups (AST and ALT values were 74 ± 16 and 70 ± 12 IU l^{-1}, respectively; the *P*-values for AST and ALT were 0.06 and 0.09, respectively). Based on these results, the dose of MTZ was set at 450 mg kg^{-1}.

The dose of MTZ was set at 15 mg kg^{-1} for experiments involving the co-administration of BSO and MTZ because it was reported that MTZ at doses of 11.4, 22.8 and 45.6 mg kg^{-1} resulted in dose-dependent increases (12- to 180-fold of the values in controls) in serum ALT activity (Mizutani *et al.*, 1999).

Administration of BSO

BSO was dissolved in water and administered intraperitoneally at a dose of 3 mmol/20 ml kg^{-1} to mice 1 h before MTZ (15 mg kg^{-1}) administration. The dose of BSO was set at 3 mmol kg^{-1} because it was confirmed in several previous studies that hepatic GSH was decreased after intraperitoneal injection of mice with BSO at a dose of approximately 3 mmol kg^{-1} (Mizutani *et al.*, 1999; Tirmenstein and Nelson, 1991; Shimizu *et al.*, 2009).

Administration of Anti-mouse IL-4 Antibodies

One hour prior to MTZ administration, the mice were administered an anti-mouse IL-4 antibody intraperitoneally (100 µg of anti-mouse IL-4 antibody in 0.5 ml of sterile PBS). As a negative control, rat IgG2a was administered (100 µg of rat IgG2a in 0.5 ml of sterile PBS).

Sample Collection and Histopathology

At 6 h after MTZ administration, the animals were sacrificed, and their plasma and livers were collected because it was reported that serum AST and ALT activities were markedly increased 6 h after MTZ administration and slightly decreased at 24 h (Mizutani *et al.*, 1999). A portion of each excised liver was fixed in 10% neutral buffered formalin, embedded in paraffin, sectioned at a 4 µm thickness and subjected to hematoxylin–eosin (HE) staining and immunohistochemical staining for MPO. The degree of liver injury was confirmed by HE staining. Neutrophil infiltration was assessed by immunostaining for MPO. After deparaffinization, liver sections were microwaved in a target retrieval solution (TRS, pH6.1, Dako) for 15 min to unmask the antigens. Then, the

